THESIS FOR THE DEGREE OF DOCTOR OF PHILOSOPHY

Photoactive EDA complexes in visible light driven aerobic oxidations

AUGUST RUNEMARK

Department of Chemistry and Chemical Engineering

CHALMERS UNIVERSITY OF TECHNOLOGY

Gothenburg, Sweden 2023

Photoactive EDA complexes in visible light driven aerobic oxidations

AUGUST RUNEMARK

ISBN: 978-91-7905-785-5

Doktorsavhandlingar vid Chalmers tekniska högskola
Ny serie nr 5251
ISSN: 0346-718X

Department of Chemistry and Chemical Engineering
Chalmers University of Technology
SE-412 96 Gothenburg
Sweden
Telephone + 46 (0)31-772 1000

Cover: *Molecules in the spotlight,* by Vilma Canfjorden

Printed by Chalmers digitaltryck
Gothenburg, Sweden 2023

Photoactive EDA complexes in visible light driven aerobic oxidations

AUGUST RUNEMARK

Department of Chemistry and Chemical Engineering
Chalmers University of Technology

Abstract

Organic synthesis driven by photochemical activation has been proven very promising in a range of scenarios within academia and industry. The emergence of photoredox catalysis has fueled an ever-growing interest in the use of visible light as a convenient energy source for a variety of radical reactions otherwise difficult to achieve. However, the use of homogeneous catalysts, based on transition metals or complicated organic dyes as the light harvesting moiety, does not come without drawbacks. Problems include the price and availability of ruthenium and iridium, and the separation and re-use of the catalysts from the products. Photochemical transformations that use simpler systems, such as catalyst-free versions or small organic molecules as photocatalysts, are therefore attractive to develop. For certain systems, one potential solution to these problems is the use of electron donor-acceptor (EDA) complexes. These complexes can form between a molecule of high electron affinity (acceptor) and a molecule of low ionization potential (donor). A key feature of the EDA complex is that it can be excited with light of a lower energy than that needed to excite the reactants on their own. The excitation of the complex can result in the formation of reactive radical species that can be harvested for further chemical reactions. EDA complexes can, with other words, be used as a convenient light-absorbing moiety to drive chemical reactions without the need of an external photocatalyst.

Oxidation reactions are a universal part of organic chemistry. The oxidants commonly used are however associated with certain drawbacks such as troublesome waste production. Oxygen obtained from the air around us is a potentially ideal alternative. The use of aerobic conditions in the combination with photoactive EDA complexes poses an interesting and underdeveloped part of photochemical transformations. In this thesis, an EDA complex approach to the synthesis of *N*-heterocycles has been investigated. The developed methods use alkylated anilines as donors and activated alkenes as acceptors to form different EDA complexes. Visible light is used to activate the complexes, and aerobic oxygen is used as the terminal oxidant to furnish the target compounds. In the first part of the thesis, new EDA complexes between dialkyl anilines and 1,2-dibenzoyl ethylenes are identified. The results show that upon excitation of the EDA complexes, 3,4-disubstituted tetrahydroquinolines can be formed in excellent diastereoselectivity and in high yields. In the second part, the identified EDA complexes are used as part of a catalytic system for the generation of α-amino alkyl radicals under aerobic conditions and under visible light irradiation. Lastly, in the third part, new EDA complexes between arylated amino acids and maleimides are identified. The photoactivation of these complexes was shown to be an efficient way of generating secondary α-amino alkyl radicals to furnish *N*-H-tetrahydroquinolines.

Keywords: EDA complex, photochemical, aerobic oxidation, visible light, organic synthesis

List of Publications

This thesis is based on the following publications:

I. Visible-Light-Driven Stereoselective Annulation of Alkyl Anilines and Dibenzoylethylenes via Electron Donor–Acceptor Complexes.
A. Runemark, S. C. Zacharias, H. Sundén
J. Org. Chem. ***2021****, 86, 2, 1901–1910*

II. Aerobic Oxidative EDA Catalysis: Synthesis of Tetrahydroquinolines Using an Organocatalytic EDA Active Acceptor.
A. Runemark, H. Sundén
J. Org. Chem. ***2022****, 87, 2, 1457–1469*

III. Overcoming Back Electron Transfer in the EDA Complex Mediated Visible Light Driven Generation of α-Aminoalkyl Radicals from Secondary Anilines.
A. Runemark, H. Sundén
J. Org. Chem. ***2023****, 88, 1, 462–474*

Publications by the author not included in the thesis:

Asymmetric Synthesis of Dihydropyranones with Three Contiguous Stereocenters by an NHC-Catalyzed Kinetic Resolution.
A. Axelsson, M. Westerlund, S. C. Zacharias, A. Runemark, M. Haukka, H. Sundén.
Eur. J. Org. Chem. ***2021****, 2021, 3657.*

Covalent incorporation of diphenylanthracene in oxotriphenylhexanoate organogels as a quasi-solid photon upconversion matrix.
D. F. Barbosa de Mattos, A. Dreos, M. D. Johnstone, A. Runemark, C. Sauvée, V. Gray, K. Moth-Poulsen, H. Sundén, M. Abrahamsson
J. Chem. Phys. ***2020,*** *153, 214705*

Polycyclizations of Ketoesters: Synthesis of Complex Tricycles with up to Five Stereogenic Centers from Available Starting Materials.
M. Kamlar, A. Runemark, I. Císařová, H. Sundén.
Org. Lett. ***2020****, 22, 21, 8387–8391*

Microwave-heated γ-Alumina Applied to the Reduction of Aldehydes to Alcohols.
B. Dhokale, A. Susarrey-Arce, A. Pekkari, A. Runemark, K. Moth-Poulsen, C. Langhammer, H. Härelind, M. Busch, M. Vandichel, H. Sundén
ChemCatChem ***2020****, 12, 6344.*

A nanofluidic device for parallel single nanoparticle catalysis in solution.
S. Levin, J. Fritzsche, S. Nilsson, A. Runemark, B. Dhokale, H. Ström, H. Sundén, C. Langhammer, F. Westerlund
Nat. Commun. ***2019****, 10, 4426*

Contribution report

Paper I
Contributed to the outline of the study. Performed the experimental work. Analyzed all the results except single crystal X-ray analysis. Wrote the manuscript.

Paper II
Formulated and designed the research project. Carried out the experimental work. Analyzed the results and wrote the manuscript.

Paper III
Formulated and designed the research project. Carried out the experimental work. Analyzed the results and wrote the manuscript.

List of Abbreviations

AcCl	Acetyl Chloride
bpy	2,2'-Bipyridine
BET	Back Electron Transfer
BHT	Butylated Hydroxytoluene (2,6-Di-*tert*-butyl-4-methylphenol)
CFL	Compact Fluorescent Lamp
CT	Charge Transfer
cy-Hex	Cyclohexyl
dtbbpy	4,4'-Di-*tert*-butyl-2,2'-bipyridine
DBE	1,2-Dibenzoylethylene
DCM	Dichloromethane
DDQ	2,3-Dichloro-5,6-dicyano-1,4-benzoquinone
DMA	*N*,*N*-Dimethylaniline
DMSO	Dimethyl sulfoxide
d.r.	Diastereomeric Ratio
EDA	Electron Donor Acceptor (complex)
EA	Electron Affinity
Equiv.	Equivalents
ES	Excited State
EtOAc	Ethyl acetate
eV	electron Volt
EWG	Electron Withdrawing Group
FDA	Food and Drug Administration
GC-FID	Gas Chromatography - Flame Ionization Detector
GS	Ground State
IP	Ionization Potential
IUPAC	International Union of Pure and Applied Chemistry
HAT	Hydrogen Atom Transfer
HOMO	Highest Occupied Molecular Orbital
KIE	Kinetic Isotope Effect
LED	Light Emitting Diode
LG	Leaving Group
LUMO	Lowest Unoccupied Molecular Orbital
MeCN	Acetonitrile
MeOH	Methanol
$MeNO_2$	Nitromethane
MsCl	Methanesulfonyl chloride
n.d.	Not Determined
Nu	Nucleophile
OMe	Methoxy
PC	Photo(-redox) Catalyst
ppy	2-Phenyl Pyridine
PT	Proton Transfer
pyr	Pyridine
RDS	Rate Determining Step
r.t.	Room Temperature
SCE	Saturated Calomel Electrode
SET	Single Electron Transfer
SOMO	Singly Occupied Molecular Orbital
THF	Tetrahydrofuran

THIQ	1,2,3,4-Tetrahydroisoquinoline
tol	Toluene
THQ	1,2,3,4-Tetrahydroquinoline
UV	Ultraviolet

Content

1. Background

The search for efficiency in the use of resources and energy prompts a constant renewal of the industry. The chemical industry in particular – with its large impact on society - is in continuous need of developing processes which use less energy, produce less waste, utilize harmless reagents, and use sustainable raw materials. In parallel, the search for new materials and pharmaceuticals prompts organic chemists to chart the unknown corners of the chemical space. Both pursuits can only be realized with research in method development

1.1. Method development

Method development of organic reactions is of particular interest in the field of organic chemistry. A method in this sense can be viewed as a recipe for a certain chemical; a series of actions carried out that drive chemical reactions to form a target compound. Methods for the synthesis of organic compounds are of high importance in the development of new medicines, materials, and commodity chemicals. Depending on factors such as scale and availability of raw materials and energy, different methods can be employed to produce the same compound. The existence of a large variety of recipes is therefore advantageous. Research in method development of organic reactions can also lead to more insight into the fundamentals behind organic reactions which in turn leads to the development of new reactions.

1.2. Light and oxygen in method development

All reactions have energy requirements. This can be in the form of heat, the introduction of a very reactive compound, or with the aid of light. Fundamentally, all chemical reactions work the same way, but electromagnetic radiation can give access to reactions that are otherwise difficult to achieve.[1] Therefore, it is useful to make a distinction between thermal and light-induced reactions. Also from a practical standpoint light is an attractive way of driving reactions. For example, the reaction control is easy by changing light intensity and wavelength.[2,3] Visible light is a rather promising source of energy and as a tool in organic synthesis.[4,5] From a safety perspective, the use of high energy UV-light, high temperatures, or highly reactive reagents is inferior compared to visible light.

With these advantages, it is desirable to design new synthetic methods that use visible light as the energy source. This is also reflected in the rapid growth of the number of such methods over the last twenty years.[6] Especially, photoredox catalysis has been the subject of great interest. In short, photoredox catalytic methods utilize a catalyst which captures the light and transforms it into chemical energy used to drive reactions. Albeit being very efficient in capturing the light, this approach does not come without its drawbacks. The catalysts used are often based on rare transition metals or complicated organic dyes. This can pose problems in terms of economy and availability. If the catalyst can be substituted with simple and cheap organic molecules, or omitted altogether, it would constitute an improvement. The work presented in this thesis is grounded in this approach. Instead of using an external photocatalyst, the inherent properties of the reactants enable the formation of photoactive intermolecular complexes that will capture the energy of the visible light to drive the reaction. The intermolecular complexes are called electron donor acceptor (EDA) complexes and constitute a promising substitute for conventional photocatalysts. During the last decade, the use of EDA complexes in organic synthesis has gained increased attention. A large variety of methods have been developed, covering many different chemical transformations, such as oxidations.[7] Oxidation reactions are universal in the synthesis and production of organic compounds at all scales.[8] Traditional oxidants based on transition metals, halogens, or highly

reactive organic compounds are troublesome in terms of waste production. Molecular oxygen obtained from the air could be an ideal alternative.[8,9] Synthetic methods that operate under aerobic conditions are therefore attractive to investigate and develop.

A family of compounds of extraordinary importance for organic chemistry is N-heterocycles. The majority of FDA approved drugs belongs to this family.[10] Research in method development targeting synthesis of compounds in this class is therefore of high interest to further develop new and better drugs. The work presented in this thesis focuses on the construction of N-heterocycles *via* functionalization of anilines using a combination of EDA complexes, visible light, and aerial oxygen.

2. Aim

The goal of the research presented in this work has been to contribute to the development of light driven synthetic methods based on EDA complexes as an alternative to conventional photocatalysts for the functionalization of anilines. In particular, the goal of the research can be formulated according to the following aims:

- Identify and characterize photoactive EDA complexes that can be used under aerobic conditions to functionalize anilines.
- Investigate the scope and limitations of the identified EDA complex mediated reactions.

3. Theory

The ultimate goal of the photochemist is to use light-matter interactions in a useful way. In order to do so, we must first consider some fundamentals. In this chapter, the basic concepts of photochemical processes will be introduced.

3.1. Light

Photochemistry is concerned with the interaction between light and matter (molecules). This interaction can occur in several different ways. However, for the chemist special types of absorption are the most useful to consider. Absorption is – according to the IUPAC recommendation – a process in which energy is transferred "from an electromagnetic field to a material or a molecular entity".[11] Within the scope of this text, light will be considered an electromagnetic wave which behaves as discrete energy packages – photons. Depending on the wavelength of the light, the photon will have a definite energy, E, according to equation (1),

$$E = \frac{hc}{\lambda} = h\nu \tag{1}$$

where h is Planck's constant, c is the speed of light in vacuum, λ is the wavelength of the light and ν is the frequency of the light.

Depending on the wavelength of the light, it will interact with the human body in different ways, and therefore we have roughly divided the spectral range into different domains depending on the wavelength. Ultraviolet (UV) light has a wavelength between 100 and 400 nm, visible light between 400 and 760 nm, and infrared light between 780 and 20 000 nm.[11]

3.2. Matter

The distribution of the electrons in a molecular entity can be described in terms of molecular orbitals.[12] For the purposes of synthetic photochemistry, the most important orbitals are the frontier orbitals i.e., the highest occupied molecular orbital (HOMO) and the lowest unoccupied molecular orbital (LUMO).[13] A process during which the electronic configuration of a molecular entity is changed to another energy state is known as electronic transition. A molecule having the electronic configuration of the lowest energy is said to be in its ground state (GS), whereas the molecule is promoted to an excited state (ES) if an electronic transition to a higher energy is occurring. In most cases that are relevant for this work, the electronic transition of highest interest can be said to correspond to the promotion of one electron from the HOMO to the LUMO of the molecule. Transitions are associated with light in such a way that when a photon is absorbed by a molecule, a transition occurs. A photon can induce an electronic transition (be absorbed) if the energy of the photon is matched by the energy difference of the two states, equation (2),

$$E_f - E_i = \Delta E = h\nu \tag{2}$$

where E_i and E_f denotes the initial and final energy levels, respectively. A practical quantity related to absorption is the absorbance, defined according to equation (3),[11]

$$A(\lambda) = \log_{10}\left(\frac{P_\lambda^0}{P_\lambda}\right) \tag{3}$$

where $A(\lambda)$ is the absorbance at a certain wavelength, P_λ^0 is the incident power of the radiation and P_λ is the transmitted power of the radiation.[11] If we plot the absorbance as a function of a quantity related to the energy of the light for a specific system (usually the wavelength), we obtain an absorption spectrum (Figure 1). In most cases for complex molecular structures, the simple picture that only the HOMO and the LUMO are involved in the GS to an ES transition is not adequate. Instead, many different transitions of varying energies are possible, involving many different molecular orbitals. Therefore, the absorption spectrum of a molecule often has several absorption maxima. The intensity of the absorption varies depending on the probability of that certain transition to occur.[14] The broad and smooth shape of the absorption peaks in the hypothetical spectrum in Figure 1 is typical for spectra obtained in a polar solvent. One reason for this is the existence of different vibrational states within each electronic state and strong solvent-solute interactions.[14]

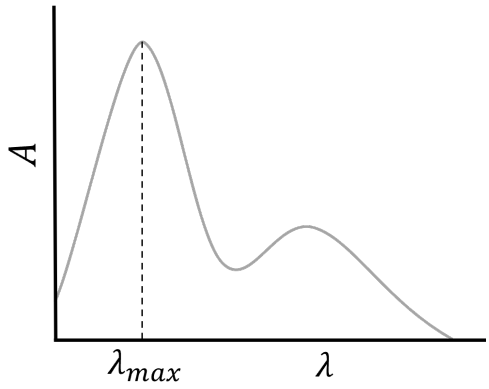

Figure 1. A hypothetical absorption spectrum, where A is the absorbance, λ is the wavelength, and λ_{max} denotes the wavelength at which the absorbance is the highest.

For a molecule in which one excitation corresponds to a promotion of an electron from the HOMO to the LUMO, the transition process can be schematically presented as in Figure 2.

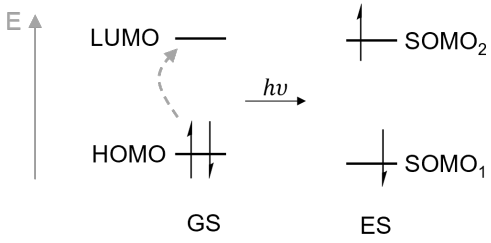

Figure 2. Schematic picture of the excitation of a molecule in terms of frontier molecular orbitals. GS = ground state, ES = excited state, HOMO = highest occupied molecular orbital, LUMO = lowest unoccupied molecular orbital, SOMO = singly occupied molecular orbital. Half arrows correspond electrons.

In the GS two electrons occupy the HOMO of the molecule. After the excitation, one electron is occupying the former LUMO and one the former HOMO. The molecule will then rearrange and relax to the lowest vibrational level of the excited state and the system will consist of two singly occupied molecular orbitals (SOMO).[14]

3.3. The fate of the excited state

After the interaction with light, what will happen to a molecule that is promoted to its excited state?

There are a range of different processes that can take place. First of all, as mentioned above, the vibrational relaxation will occur. We will assume that the following processes occurs from this state. Now the - still highly energetic - excited state can undergo different pathways of decay: direct relaxation to the ground state *via* the emission of a photon (fluorescence) or isoenergetic transition to another electronic state (internal conversion or intersystem crossing), and from there further relaxation *via* VR or emission to finally reach the GS again.[11,14]

3.4. Photochemical transformations

Regardless of how intriguing the processes associated with the excitation and relaxation of a molecule in its own right might be, to make chemistry bonds must break or form. Let us therefore consider the different destructive processes that can occur from the excited state, processes of the type described by equation (4),

$$A + h\upsilon \rightarrow A^* \rightarrow B \qquad (4)$$

where A* is an excited state of A, and B is a molecule non-identical to A. A classic example of such a photoreaction is the photoisomerization of alkenes, Figure 3.[15]

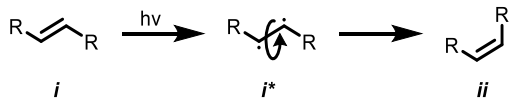

Figure 3. Alkene isomerization reaction.

In this reaction, the excitation of the alkene ***i*** to its ES (***i****) results in the weakening of the double bond due to the promotion of one electron from the bonding HOMO to the antibonding LUMO. This facilitates rotation along the σ-bond, enabling formation of the opposite isomer (***ii***). A reaction with a high energy barrier on the GS energy surface is thus possible on the ES energy surface by using the fact that the ES surface has a different shape. This is the fundamental principle that makes the photochemical reactions so compelling.

The photoisomerization of alkenes is relevant for the results reported later in this thesis, but of more importance is the concept of photoinduced electron transfer – the formation of charge separated states as the result of light irradiation, introduced in the following section.

3.5. Electron transfer

The transfer of one electron from one species to another is a fundamental phenomenon in chemistry. This superficially simple process has been the subject of immense research during the last century, and a large theoretical framework has been developed.[16] Consider a hypothetical case of the single electron transfer (SET) from an electron donor (D) to an electron acceptor (A) according to equation (5).[17]

$$D + A \rightarrow D^{\cdot+} + A^{\cdot-} \qquad (5)$$

In this reaction, D is being oxidized and A is being reduced. The process in whole is as a redox reaction. In terms of frontier molecular orbitals, this process can be schematically represented as in Figure 4.

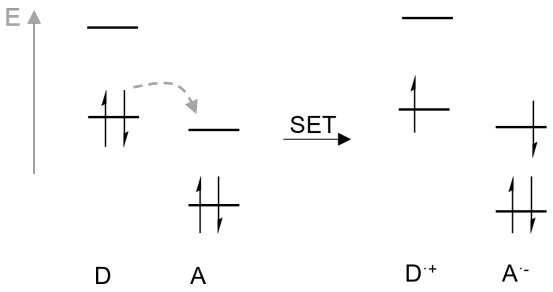

Figure 4. Single electron transfer from HOMO of D to LUMO of A.

The energy change of the reaction involves the energy required to completely remove one electron from D, and the energy associated with the gain of one electron to A. Considering a reaction in gas phase, these two energies are nothing but the ionization potential (IP) of D and the negative IP of A^- (also referred to as electron affinity, EA). Thus, the total energy change of the combined half-reactions can be expressed according to equation (6).

$$\Delta E = IP_D - EA_A \tag{6}$$

This expression gives a very simple picture of what fundamentally drives the electron transfer. However, since most chemistry relevant to this work is carried out in a solvent, it cannot directly be applied due to the influence of solute-solvent interactions. Therefore, the experimentally determined electrode potentials are more useful. The electrode potential, E, is a quantity that gives information about the energy required to reduce a certain compound, compared to a reference compound. It is denoted as $E(A/A^{\cdot-})$ for the half reaction $A + e^- \rightarrow A^{\cdot-}$.* This potential can validly be compared to other potentials if the same reference electrode is used.

The Gibbs free energy change of a SET between two neutral species D and A, in terms of electrode potentials, can in a simplified manner be formulated according to equation (7),[11,16,17]

$$\Delta_{ET}G^0 = N_a e\left[E^0\left(\frac{D^{\cdot+}}{D}\right) - E^0\left(\frac{A}{A^{\cdot-}}\right)\right] + \frac{N_a(z_{D^{\cdot+}} + z_{A^{\cdot-}})e^2}{4\pi d\varepsilon_0\varepsilon_s} \tag{7}$$

where N_a is Avogadro's constant, e is the elementary charge, Z_i is the charge of species i, d is the distance between the resulting ions, ε_0 is the dielectric constant of vacuum and ε_s is the relative dielectric constant of the solvent. The second term in the equation – called electrostatic work term - illustrates the importance of the solvent for the driving force of electron transfer processes. However, for cases when reactions are carried out in a solvent with a high dielectric constant, this part of the equation can usually be omitted due to its small contribution. Noteworthy here is that nothing has been stated about the mechanism *via* which the electron transfer occurs, the energy change only takes in to account the initial and final states.

* Note that this thesis will follow the convention of not using the terms oxidation of reduction potential.[11] Thus, for the oxidation of D to $D^{\cdot+}$ the relevant electrode potential is $E(D^{\cdot+}/D)$, referring to the process $D^{\cdot+} + e^- \rightarrow D$.

Once the SET has occurred, other processes of varying nature will take over. These are of course of utmost importance if we would want to use the electron transfer in a practically useful reaction. One major pathway for many electron transfer processes is the back electron transfer (BET) process in which a SET occurs again, but in "reverse", reforming D and A. This process must be suppressed to favor other, synthetically productive, pathways. This can be achieved using different approaches, of which irreversible fragmentation of the radical ions is one.

3.5.1. Photoinduced electron transfer

With the background to electron transfer laid out, we can turn our attention back to photoinduced processes. Analogous to D and A in their ground states, associated with their excited states are the excited state electrode potentials. These can be used to estimate the outcome of electron transfer processes involving D* or A*.These excited states can part-take in redox reaction with ground state entities according to equation (8) and (9).[17]

$$D^* + A \rightarrow D^{\cdot+} + A^{\cdot-} \tag{8}$$

$$D + A^* \rightarrow D^{\cdot+} + A^{\cdot-} \tag{9}$$

The excited state potentials can rarely be measured directly. Instead, the ground state potential and the energy of the relevant excited state needs to be combined to estimate this. This energy is in this case usually denoted $E_{0,0}$. The 0-0 index refers to the lowest vibrational levels of the ground and excited states. Added to equation (7), an expression for the free energy change of photoinduced electron transfer can be written according to equation (10):[11]

$$\Delta_{ET}G^0 = N_a e\left[E^0\left(\frac{D^{\cdot+}}{D}\right) - E^0\left(\frac{A}{A^{\cdot-}}\right)\right] + \frac{N_a(z_{D^{\cdot+}} z_{A^{\cdot-}})e^2}{4\pi d\varepsilon_0\varepsilon_s} - \Delta E_{0,0} \tag{10}$$

Photoinduced electron transfer is of fundamental importance within the field of light mediated organic reactions. The formed charged species $D^{\cdot+}$ and $A^{\cdot-}$ can in a variety of ways be used to carry out reactions. Since they are typically the result of a SET between closed shell species, they are radicals. One subgroup of light-driven reactions is especially relevant to mention here: photoredox catalysis.

3.6. Photoredox catalysis

Of fundamental importance for the development of synthetically useful visible light driven organic synthesis is the development of photoredox catalysis.[1,6,18] Methods belonging to this subgroups rely on the excitation of a photoredox catalyst (PC), which then can act either as an electron donor or acceptor when interacting with D or A (Figure 5).[6,19] Which mode of reactivity is likely to operate can be rationalized in terms of electrode potentials, see equation (10). Alternatively, the excitation energy can be transferred to form the excited state of the substrate, although this possibility will not be considered herein.

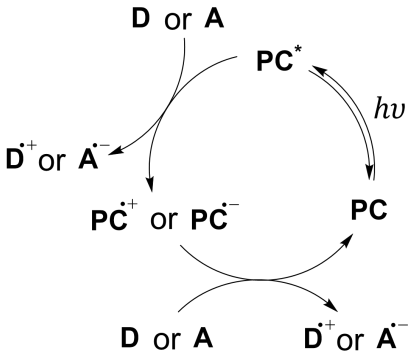

Figure 5. Photoredox catalysis cycle. PC = photoredox catalyst, D = electron donor, A = electron acceptor.

After the substrate has been oxidized or reduced, the formed radicals take part in any suitable radical reaction, depending on the system. Meanwhile, the reduced or oxidized catalyst will return to the initial state *via* the interaction with another redox active species, closing the catalytic cycle. A wide variety of photoredox catalysts exists. In Figure 6 the structures of some of the most common of all catalysts are presented. These include both transition metal complexes ($[Ir(dtddpy)(ppy)_2]^+$ and $[Ru(bby)_3]^{2+}$) and organic dyes (acridinium salts and Eosin Y).[6]

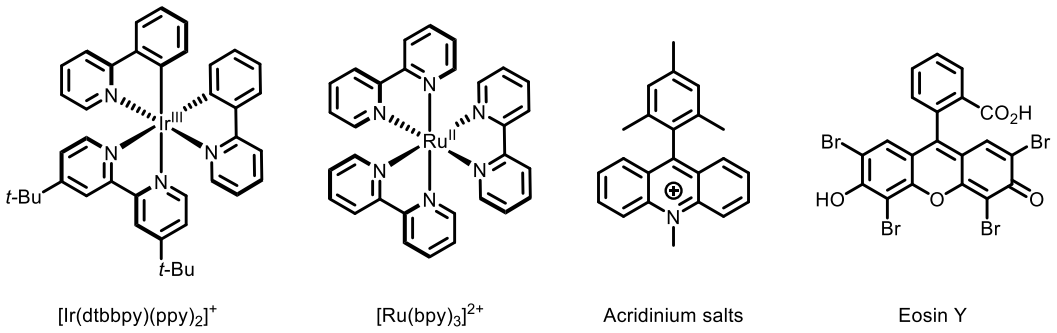

Figure 6. Structures of some common photoredox catalysts.

One of the benefits of photoredox catalysis is that compounds not absorbing in the visible range of the spectrum (true for most common small organic molecules) still can be modified by visible light. It is also a convenient way of producing radical species that otherwise require rather harsh conditions to form. However, several drawbacks with using a photoredox catalyst can be identified. The traditional metal complexes are based on transition metals such as ruthenium and iridium which are rare in the earth's crust.[20] This can cause problems in the availability and sustainability of these catalysts. Organic dyes on the other hand are easier and cheaper to obtain, but still requires multistep synthesis. Like homogeneous catalysts in general, both transition metal based and purely organic PCs can also be difficult to separate from the product mixture and reuse.[21] For these reasons alternative methods driven by visible light without the need of photoredox catalysts, or methods using simpler organic catalysts, are still attractive.

3.7. Electron Donor Acceptor complexes

Another approach to enable photochemical activation of compounds not absorbing in a certain region of the spectrum is via EDA complexes. These entities are – as the name implies - the result of an interaction between an electron donor and an electron acceptor, both in their ground states.[22,23] Their electrode potentials are such that a ground state electron transfer is not favorable. However, orbital mixing of the HOMO of the donor and LUMO of the acceptor is occurring. Simply put, this orbital mixing gives rise to two new orbitals, which opens the possibility of a new

electronic transition. In the electromagnetic spectrum this is observed as a new absorption which is not present in either the donor or the acceptor separately. The new absorption band associated with the EDA complex is called a charge transfer (CT) band, see Figure 7.

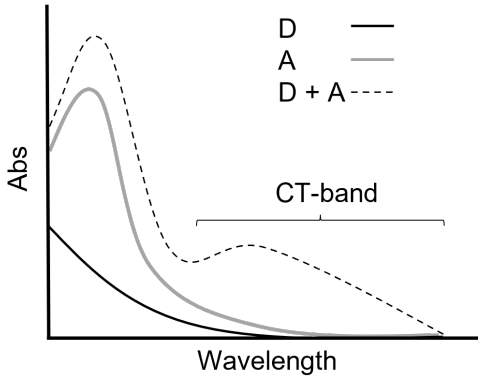

Figure 7. Hypothetical UV-vis spectrum of an EDA complex and its constituents. The thick black line corresponds to the absorption of the donor (D), the thick grey line corresponds to the absorption of the acceptor (A), and the dashed black line corresponds to the resulting absorption of the mixture of D, A and the EDA complex formed when the donor and acceptor are mixed in solution.

As the name implies, this transition gives rise to a state where electronic charge is transferred from the donor to the acceptor forming an ion pair.[11,24] The energy required to excite the EDA complex is typically lower than required to excite either D or A separately, hence the CT band is observed towards longer wavelengths in the absorption spectrum.[7,23] Therefore, visible light can often be used to excite EDA complexes formed between species which separately only absorbs in the UV region. The practical implication of this is the same as for photoredox catalysis: visible light can be used to invoke chemical modifications of compounds not absorbing in the visible region. Equation (11) describes schematically the process of EDA complex formation and the generation of the charge separated state. EDA complexes are also characterized by their association constant, K_a, according to equation (*12*).[23] This constant can be determined by titration experiments. For typical EDA complexes between organic compounds, the K_a is in the range of 0.1 – 1 M^{-1}.[23]

$$D + A \overset{K_a}{\rightleftharpoons} DA \overset{h\nu_{CT}}{\rightleftharpoons} D^{\cdot+}A^{\cdot-} \longrightarrow D^{\cdot+} + A^{\cdot-} \tag{11}$$

$$K_a = \frac{[DA]}{[D][A]} \tag{12}$$

The energy of the CT transition ($h\nu_{CT}$) is ultimately the energy needed to transfer one electron from the donor to the acceptor, and as such equation (2) and (6) can be combined to describe the CT energy in equation (13).[25]

$$h\nu_{CT} \propto IP_D - EA_A \tag{13}$$

The overall energy change for the process in equation (11), also involves e.g., solvation energies, and can be described according to equation (*7*).

3.7.1. EDA complexes in organic synthesis

Given their high importance for the work in this thesis, a short historical overview of EDA complexes and their use in organic synthesis is relevant. Prototypical early examples of intermolecular interactions classified as EDA complexes include mixtures of halogens and aromatic hydrocarbons. For example, the appearance of intense absorption bands in the UV region upon mixing iodine and diethyl ether was investigated and concluded to be a result of a 1:1 iodine-ether complex.[26] Although the observed phenomena sparked an interest in many chemists and lead to the development of electron transfer theory, the use of EDA complexes in synthesis did not appear until the 1970's.[23] Such early examples typically concerned the use of stoichiometric complexes leading to coupling or substitution reaction upon excitation.[23] As an example, Kochi and co-workers reported the photochemical addition reaction of tetramethyl tin over the double bond of tetracyanoethylene in 1979 (Scheme 1a).[27] The reaction is proposed to proceed *via* the activation of complex **EDA-1**, formed between the electron deficient alkene **2** and the tetramethyl tin **1**.[27] In a following paper in 1987, the same group reported complex **EDA-2** formed between 4'-methyl anisole and tetranitromethane (Scheme 1b).[28] Irradiation with visible light resulted in the aromatic nitration of the methyl anisole.

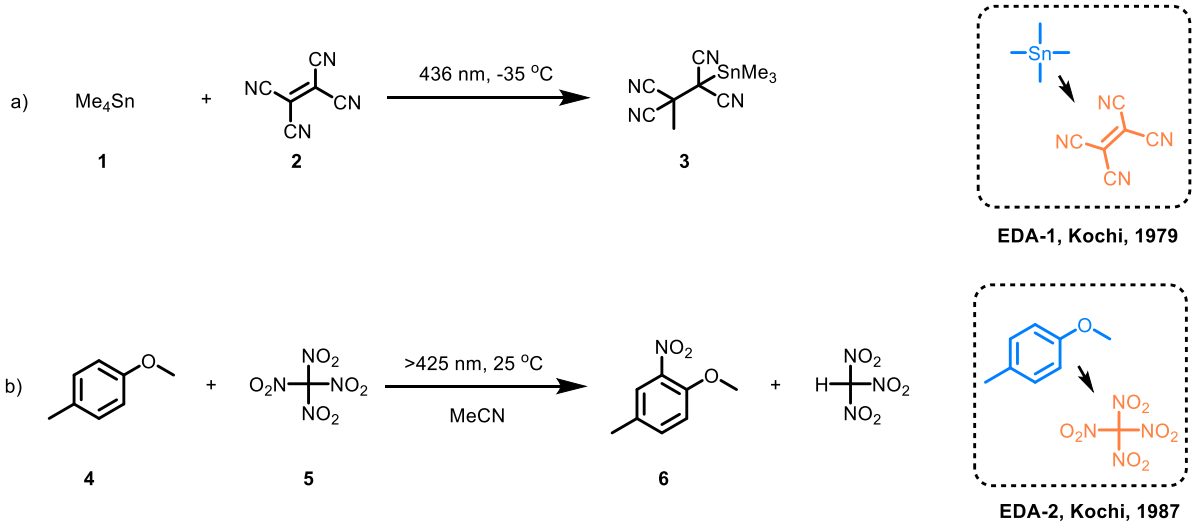

Scheme 1. a) Photoreaction between tetralkyl tin and tetracyano ethylene proceeding via an EDA complex, reported by Kochi and co-workers[27] b) Photochemical nitration of methyl anisole via activation of an EDA complex, reported by Kochi and co-workers.[28]

Between the years 1990 and 2020, a wide range of different approaches to utilize EDA complexes in synthetic organic chemistry have been developed to include, arylations, stereoselective alkylations, oxidative annulations, and acylations.[7,23,29–32]

By large, the development of organic synthesis methods proceeding *via* the photoactivation of EDA complexes has followed in the footsteps of photoredox catalysis.[7] Unsurprisingly so, given that the radical chemistry outside of the actual photoredox catalytic cycle in many cases is identical. Development of many successful methods comes from the observation of a background reaction in the absence of any catalyst. This, coupled to the increasing availability of high-power light emitting diodes (LED) with narrow emission bands, has driven the development of the field. As a key example of the serendipitous discovery of EDA complex driven methods can be mentioned a pioneering study by Chatani and coworkers from 2013 (Scheme 2a).[29] The work initially aimed at using an iridium-based photoredox catalyst in combination with diaryliodonium salts (**8**) as aryl

radical precursors. Coupled with aromatic heterocycles, an aryl-aryl coupling product (**9**) could be achieved. However, during the investigation of different heterocycles the authors observed that the reaction proceeded without the need of a catalyst if pyrroles (**7**) were used as substrates. The rationale presented was the formation of EDA complexes between the nucleophilic pyrrole and the electrophilic iodonium salts (**EDA-3**).[29]

Another example from the same year concerns the enantioselective α-benzylation of aldehydes by benzyl bromides (Scheme 2b).[30] As a background, in 2010 MacMillan and co-workers achieved this transformation for the first time using a combined organo- and photoredox catalyst system (Scheme 2b, path A).[33] In the first step of the organocatalytic cycle, the enamine **12** is formed through a condensation between aldehyde **10** and an pyrrolidine-based organocatalyst **11**. An electrophilic benzyl radical, formed from the SET reaction between benzyl bromide **13** and an iridium-based PC in its excited state, then adds to the double bond of the enamine **12**. After oxidation of the intermediate α-aminoalkyl radical by the action of the PC in its oxidized form, intermediate iminium ion **14** is formed. Finally, after hydrolysis, the α-benzylated aldehyde **15** and the regenerated catalyst **11** are formed. The scope of the reaction was inherently limited to electron deficient benzyl bromides due to the initial SET from the iridium photoredox catalyst and the bromide. Subsequently, in 2013, the Melchiorre group managed to develop a method for the same transformation but without the need of a photoredox catalyst (Scheme 2, path B).[30] Instead, the inherent electronic properties of the reactants **12** and **13** were exploited in the formation of photoactive EDA complexes. In this EDA complex, (**EDA-4**), the electron rich enamine acts as the donor, and the benzyl bromide as the acceptor.

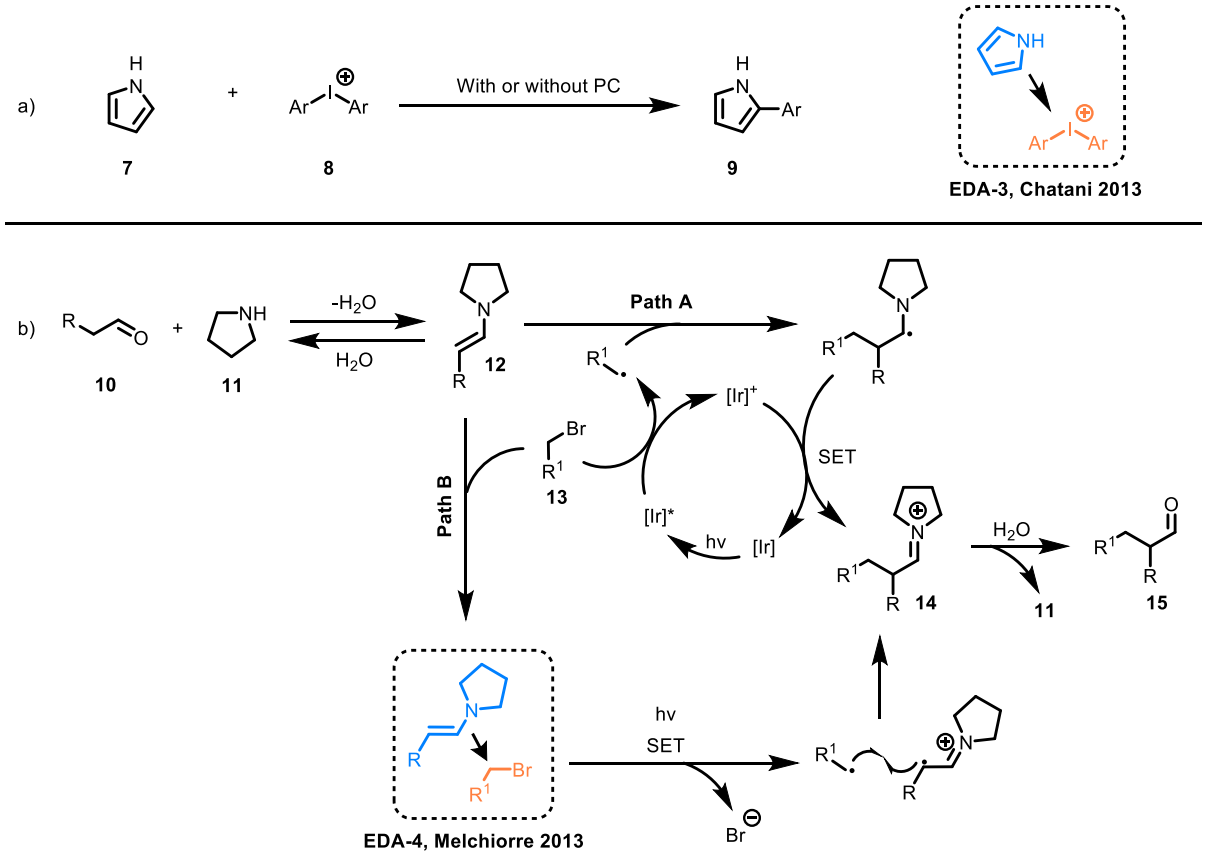

Scheme 2. Two examples of the use of EDA complexes in synthesis; a) arylation of heterocycles reported by Chatani and co-workers in 2013;[29] b) organo-photocatalytic enantioselective benzylation of aldehydes developed by MacMillan and co-workers in 2010 (path A),[33] and an EDA complex approach to the enantioselective benzylation of aldehydes developed by Melchiorre and co-workers in 2013 (path B).[30]

Some generally useful insights about methods using photoactivation of EDA complexes can be gained by looking at the two 2013-papers and letting them serve as typical examples. Firstly, they illustrate two different approaches in the design of EDA complex mediated reactions: stoichiometric (Chatani)[29] and catalytic (Melchiorre).[30] Originally, many of the investigated reactions proceeded *via* the activation of stoichiometric complexes between reactants that both end up in the product. The work by Melchiorre however, shows that we can also use a catalytic approach, expanding the synthetic power of EDA complexes significantly.

Another lesson that can be drawn from the two examples is the importance of designing systems to avoid the unproductive BET pathway. In the paper by Chatani, the aryliodonium salt fragments quickly after SET, forming iodobenzene and an aryl radical.[29] This fragmentation is irreversible and therefore competes efficiently with the BET. Likewise, the benzyl bromide forms a reactive radical anion after SET which quickly fragments to the more stable benzyl radical and a bromide anion, driving the reaction forward.

3.8. Aerobic Oxidations

Oxidation reactions are among the most important and commonly used organic transformations.[34] As such, many different oxidants have been developed, depending on the different chemical and practical demands. Suitable oxidants are in many cases based on transition metals, halogens, or peroxides. As in any redox reaction, for the substrate of interest to be oxidized, something must be reduced, i.e., a stoichiometric number of electrons must be taken care of by an electron acceptor. Therefore, if the oxidant is based on a metal or another high molecular weight species, the mass of waste will inevitably be large – and are in many cases also toxic or difficult to dispose of. A terminal oxidant that has low molecular weight, is easy to handle, is non-toxic, and generates non-toxic byproducts is for obvious reason superior. Dioxygen (O_2) is, as the name might imply, the prototypical oxidant. Constituting a fifth of the earth's atmosphere it is also arguably the most common oxidant that we have. As it turns out, it also might be the most beneficial oxidant, in terms of atom economy and waste production, as the byproduct from its full reduction in many cases is water. However, it goes without saying that scaling up reactions involving O_2 in combination with flammable organic solvents or reactants has its inherent safety risks.[8]

Albeit being all around us, we are not consumed at any appreciable rate by the oxygen. This is due to some special features of the bonding in the dioxygen molecule, making the activation barrier for its reduction quite high although the thermodynamic drive is strong.[35] This fact also makes its use as an oxidant in organic reactions somewhat challenging. O_2 is, in its ground state, considered a diradical, but has a high energy barrier compared to similar oxygen-centered radicals for typical radical reactions such as hydrogen atom transfer (HAT).[35] On the other hand, once the O_2 has been "activated" to form other oxygen centered radicals (such as $HO_2^{\cdot}$ or $O_2^{\cdot-}$), radical chain mechanisms can unleash the full power of the molecules oxidative potential in an uncontrolled manner. Therefore, the challenge is the balance between these extremes. Many systems using aerobic O_2 as the terminal oxidant have been developed. One of the more elegant can be found in our respiratory electron transport chain, and has been the model for many synthetic versions based on different transition metals.[8,34]

In the context of photoredox catalysis, O_2 has been used as the terminal oxidant in a number of examples.[36,37] A common pathway is the interaction between the photoredox catalyst and molecular oxygen in a SET manner, forming the highly reactive $O_2^{\cdot-}$. This can act either as a way of ensuring catalyst turnover, or the formed oxygen radical anion can react further in productive ways to drive selective oxidations.

Among oxidative reactions driven by the light activation of EDA complexes, O_2 has been used as the terminal oxidant in several cases.[31,38–40] An example especially relevant for this work is the aerobic oxidative annulation between dialkyl anilines and maleimides, reported by Sundén and co-workers in 2018, Scheme 3.[31]

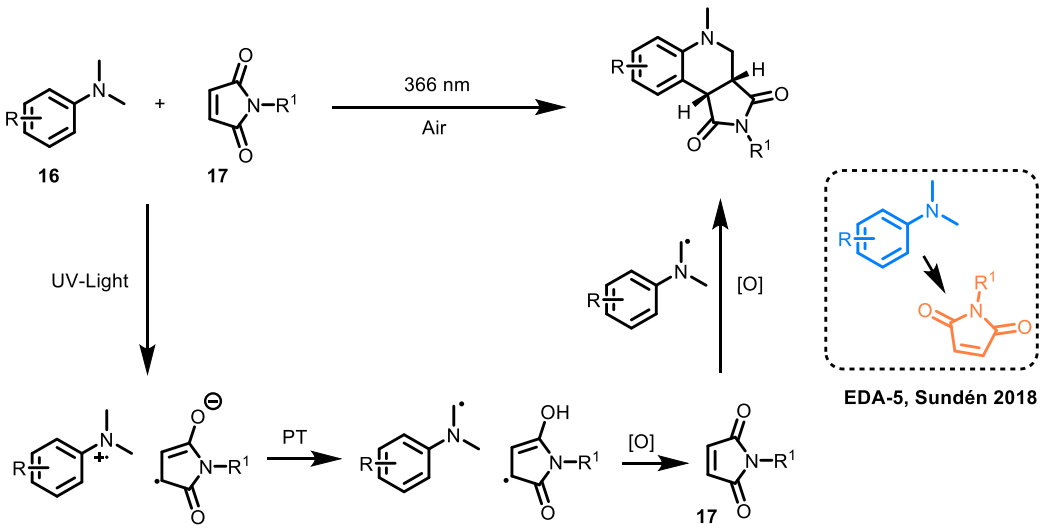

Scheme 3. Aerobic oxidative annulation between dialkyl anilines and maleimides driven by photoactivation of EDA complexes.[31]

In this example, excitation of an EDA complex (**EDA-5**) formed between dialkyl anilines (**16**) and maleimides (**17**) generates an α-aminoalkyl radical and a maleimide radical. Dioxygen is then thought to serve as the oxidant for the regeneration of maleimide from the maleimide radical. This step is crucial to allow for the α-aminoalkyl radical to add to maleimide to yield the final product under oxidative conditions. In this example, UV light is used as the irradiation source and visible light was shown to be less efficient.[31,41]

3.9. Functionalization of Anilines

The work in this thesis concerns the combination of photoactive EDA complexes and aerobic oxidation. The focus is on oxidative α-functionalization of amines (Scheme 4). Due to their low electrode potential, amines can be combined with a range of electron acceptors to yield an amine radical cation *via* SET (**18** in Scheme 4).[42] Depending on the substituents and conditions, different pathways can then lead to the final product. If a suitable leaving group (LG) is situated in the α-position, the α-bond can break either mesolytically, forming the α-amino alkyl radical (**19**), or homolytically forming the iminium ion (**20**). The radical **19** can also be further oxidized to form **20**.

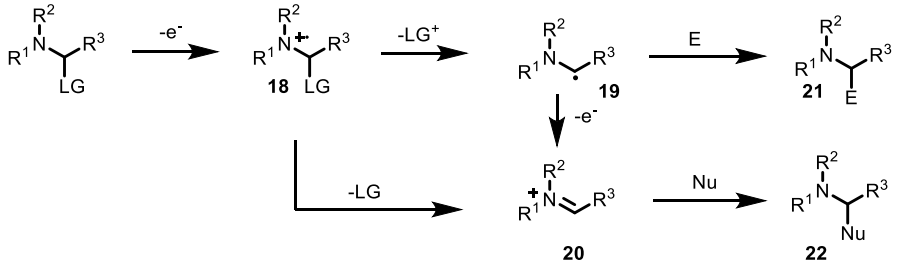

Scheme 4. Generalized oxidative functionalization of amines. LG = leaving group, E = electrophile, and Nu = nucleophile.

Due to the electron donating properties of the nitrogen lone pair, the α-amino alkyl radical is nucleophilic and can be combined with a suitable electrophile to yield a final product **21**.[42] In contrast, the iminium ion **20** is electrophilic and reacts with a nucleophile, resulting in products **22**. Oxidative functionalization can therefore be used to introduce a range of different – both nucleophilic and electrophilic – functional groups in the α-position of the amine.

Generally, the LG is a group that can stabilize a positive charge (such as H, Me_3Si or CO_2^-).[42] The α-protons are rendered acidic upon oxidation of the amine and thus deprotonation to the α-amino alkyl radical can easily be achieved in the presence of a suitable base.[42,43] In cases were a better leaving group than a proton is needed, installation of both silyl groups and carboxylic acids have successfully lead to radical formation.[42]

3.9.1. Photochemical functionalization of amines

In principle, any electron acceptor with a suitable electrode potential could be used to oxidize the amine and accomplish α-functionalization. Many thermal systems have been developed based on transition metals such as ruthenium, copper, iron or manganese in combination with terminal oxidants such as molecular oxygen, peroxides or organic oxidants†.[44,45] However, with the development of photoredox catalysis a new window of opportunity opened and functionalization of amines could be achieved efficiently using light.[46]

As an example of this, one pioneering method developed by Stephenson and co-workers in 2010 (Scheme 5) can be mentioned.[47] Here, the tetrahydroisoquinoline (THIQ) **23** is oxidized by an iridium photoredox catalyst in its excited state, followed by a HAT to an oxyradical to form the iminium ion **24**. Nitromethane then intercepts **24** to form the final coupling product **25**. The approach has since been extended to a range of different amines, photoredox catalysts, and nucleophiles.[48]

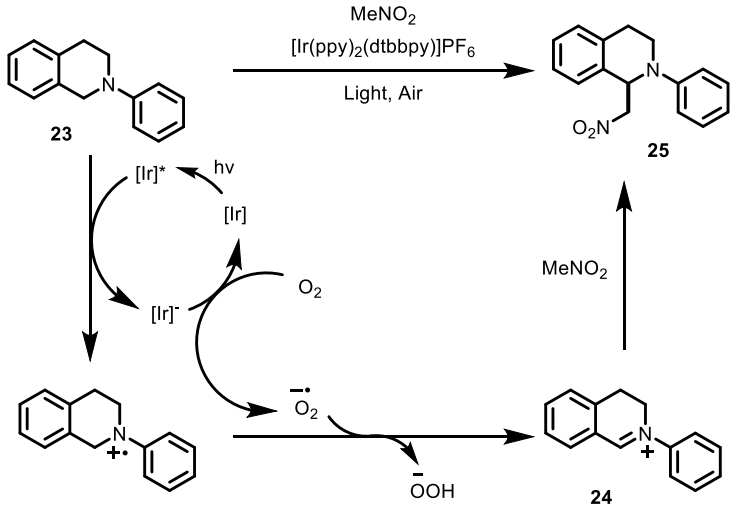

Scheme 5. Example of aerobic oxidative functionalization of amines via photoredox catalysis reported by Stephenson and co-workers in 2010.[47]

† Such as 2,3-Dichloro-5,6-dicyano-1,4-benzoquinone (DDQ)

3.9.2. EDA complexes in amine functionalization

As mentioned above, in the footsteps of the photoredox methods seems to come the EDA complex-based methods. This is also true for amine functionalization. The transformation shown in Scheme 3, was first reported using $[Ru(bby)_3]Cl_2$ as the PC in 2012 and until the catalyst-free version was developed, several different photocatalytic systems were reported.[49–54] For the transformation shown in Scheme 5, it took until 2015 when a photocatalyst-free version was developed.[55] In this case, the authors postulated several different pathways, one of which includes an EDA complex formed between the THIQ **23** and the oxidant $BrCCl_3$. Expanding the scope from THIQ to alkyl anilines in general, several methods relying on their properties as donors in EDA complexes have been developed.[31,40,41,56–61] However, the combination of aerobic oxidation and photoactivation of EDA complexes to achieve α-functionalization of alkyl anilines is still underdeveloped. In the following sections, three papers with the aim to address this lack of methods will be presented.

4. Annulation of Alkyl Anilines and Dibenzoylethylenes via Electron Donor–Acceptor Complexes (Paper I)

4.1. Introduction

Construction of N-heterocyclic compounds is one of the most fundamental tasks of organic chemistry, and their importance within the pharmaceutical industry cannot be overstated.[62] In the pursuit of developing new and better pharmaceuticals to meet the demands of society, new methods for synthesizing both known and novel compounds of this family is of never ending interest. A subclass of the N-heterocycles is the 1,2,3,4-tetrahydroquinolines (THQs). The core structure can be found in a variety of biologically active compounds (Figure 8).[63,64] Examples include molecules with antiviral,[65–67] antibiotic,[68,69] and cytotoxic activity.[70,71] A wide variety of methods used to furnish the THQ scaffold has been developed, such as the Povarov reaction.[64] Oxidation of the THQ core yields the parent quinoline (see caspase-3 inhibitors in Figure 8), another heterocyclic core structure with a central role in medicinal chemistry.[72]

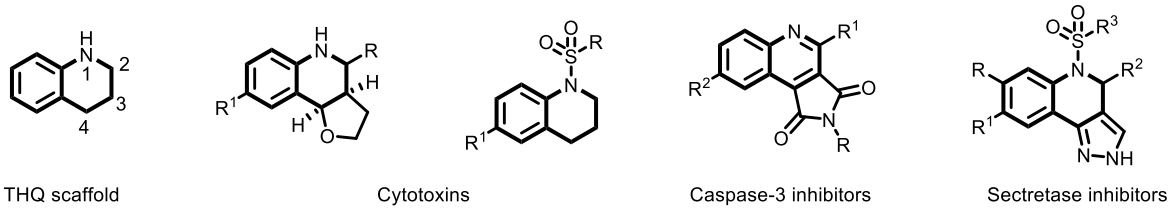

Figure 8. The THQ scaffold and biologically active members thereof.

In addition to thermal conditions, several methods relying on photoexcitation can be found in the literature.[50,53,54,73–75] Typically, a photoredox catalyst is needed to carry out the oxidative annulation. However, the need for photoredox catalysts comes with certain drawbacks, such as the use of scarce transition metals, troublesome purifications or difficulties in recovering the catalyst. Therefore, development of catalyst-free methods leading to the desired THQ scaffold is highly attractive. Previous findings from our research group concerning EDA complexes between maleimides and dialkyl anilines (Scheme 3) sparked the interest to further investigate the synthetic power of EDA complexes in the formation of THQ derivatives.[31]

It was hypothesized that the method could be expanded to other activated alkenes than maleimides, such as the 1,2-dibenzoyl ethylenes (DBE). This would give access to novel 3,4-disubstituted THQ.

4.2. Results and discussion

Initially it was observed that when 4,*N*,*N*-trimethylaniline **26** and the DBE **27** were mixed in solution, an immediate color change took place. When measuring the absorbance of the different samples an increased bathochromic absorbance of the solution was confirmed indicative of the formation of an EDA complex (Figure 9).

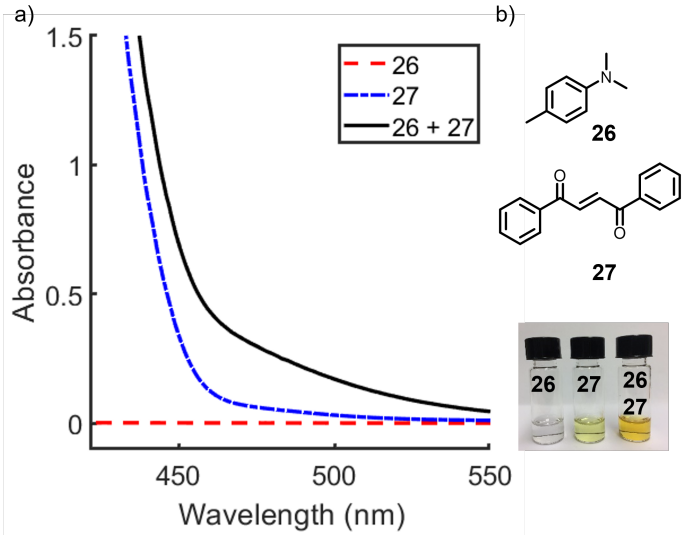

Figure 9. a) Absorbance of the components **26** and **27**, and their mixture in 1,4-dioxane; b) structures of **26** and **27**, and photographs showing the color change when mixing the components.

Upon irradiation of the mixture at room temperature and under ambient atmosphere, the formation of the annulation product **28** could be observed in 25% yield (Table 1, entry 1). Initially the reaction was carried out in acetonitrile, but after a brief investigation it was concluded that 1,4-dioxane was the best choice available, giving the product in 65% yield (Table 1, entry 8). Adding acetic acid as co-solvent increased the yield even further to a final optimized yield of 73% (Table 1, entry 16). Increasing the reaction time from four hours did not result in higher yields, neither did running the reaction under an atmosphere of oxygen – in an attempt to promote the oxidative cyclization. Other oxidants, such as potassium persulfate worked to some degree, however resulting in lower yields of the desired product (Table 1, entry 12 and 13).

The choice of irradiation source is of utmost importance when designing photochemical transformations; the spectral overlap between the emission of the lamp and the absorbance of the reaction mixture must be significant enough to promote the reaction.[‡] In the case of this transformation, a "white" household compact fluorescent lamp (CFL) with broad emission in the visible range, was chosen to cover the full absorption region of the reaction mixture. A major drawback with this approach is, however, that selective excitation is not achieved. Therefore, it is difficult to determine what absorbing species contribute to the product formation. For this reason, it is advisable to also run the reaction using LED lamps with narrower emission bands. In the reaction investigated herein, it was concluded that blue LED (with an emission maximum of 465 nm) could efficiently be used, suggesting that excitation of the CT band of the EDA complex is important for the reaction outcome.

‡ Reflected in the first law of photochemistry, attributed to Grotthuss and Draper, light must be absorbed in order for a photochemical reaction to occur.[108]

Table 1. Optimization of the reaction conditions for the oxidative annulation reaction.

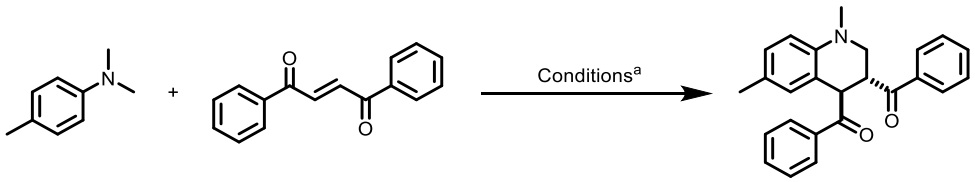

26 **27** **28**

Entry	Solvent	Light source	Yield **28** (%)[b]	d.r.[c]
1	MeCN	White CFL	25	>25:1
2	MeOH	White CFL	14	>25:1
3	THF	White CFL	29	>25:1
4	EtOAc	White CFL	17	>25:1
5	DCM	White CFL	40	>25:1
6	1,2-Dichloroethane	White CFL	41	>25:1
7	1,2-Dimethoxyethane	White CFL	32	>25:1
8	1,4-Dioxane	White CFL	65	>25:1
9	1,4-Dioxane	White CFL	30[d]	>25:1
10	1,4-Dioxane	White CFL	0[e]	-
11	1,4-Dioxane	White CFL	12[f]	>25:1
12	1,4-Dioxane	White CFL	37[g]	>25:1
13	1,4-Dioxane/water (2:1)	White CFL	47[g]	>25:1
14	1,4-Dioxane	Blue LED (450 nm)	23	>25:1
15	1,4-Dioxane	White CFL	68[h]	>25:1
16	**1,4-Dioxane**	White **CFL**	**73[i]**	**>25:1**
17	1,4-Dioxane	UV-CFL (365 nm)	30	>25:1
18	1,4-Dioxane	-	0[j]	-
19	1,4-Dioxane	Blue LED (465 nm)	60[i, k]	>25:1

a) Reaction conditions: **26** (0.7 mmol) and **27** (0.1 mmol) in 3 mL solvent irradiated with two 15 W CFLs at room temperature for 4 hours; b) determined by ^{1}H NMR using durene as internal standard; c) d.r. = diastereomeric ratio, determined by ^{1}H NMR of reaction mixture; d) 4 equiv. amine; e) under argon; f) under O_2; g) $K_2S_2O_8$ (2 equiv.) used as an additive; h) acetic acid (30 equiv.) used as co-solvent; i) acetic acid (80 equiv.) used as co-solvent; j) reaction performed in the absence of light; k) irradiated for 12 hours.

Proceeding with the conditions from Table 1, entry 16, the effects of substitution on the DBE reaction partner was investigated, Scheme 6. Generally, it was observed that electron donating groups resulted in a lower yield of the desired product. Examples are the *p*-,*m*-dimethyl and *p*-methoxy substituted DBEs, giving the products **37** and **33** in 46% and 50%, respectively. This might be an effect of either a weaker EDA complex or lower tendency for SET from the aniline

to the alkene. Likely a combination of these factors. The fact that no selectivity was observed when an unsymmetrical DBE was subjected to the reaction conditions (Scheme 6, **38**) is an indication that the addition of the α-amino alkyl radical to the alkene is not very sensitive to electronic effects. Simple *p*-halogen substituted DBE gave comparable, or slightly higher yield than the unsubstituted compound. Again, this could be a result of the thermodynamics of the EDA complex formation or the SET efficiency. However, DBE substituted with the strongly withdrawing trifluoromethyl groups resulted in a very low yielding reaction. This could be an outlier, and the low yield can be attributed to an unselective reaction with many uncharacterized by-products.

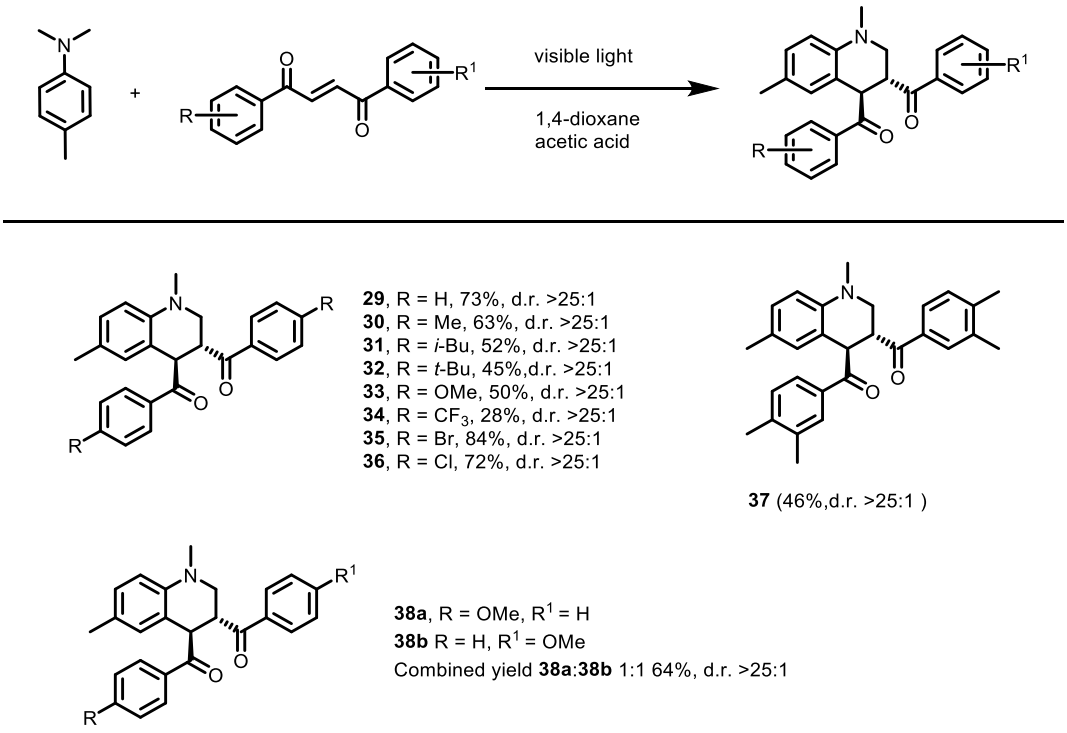

Scheme 6. Reaction scope with respect to the DBE reaction partner. Reaction conditions according to Table 1, entry 16. n.d. = not determined, d.r. = diastereomeric ratio.

Different *N*,*N*-dialkyl anilines were also tested in combination with unsubstituted DBE to yield the products **39**-**50** (Scheme 7). Substituents on the aromatic ring of the aniline core significantly affected the reaction outcome. Maybe unsurprisingly so, considering the impact on the electrode potential, and thus the SET process. The presence of the mildly electron withdrawing bromide in the *p*-position limited the yield of compound **45** to 24% under the current conditions. Steric effects were also prominent, reflected in the low yields of compounds **40** and **41**.

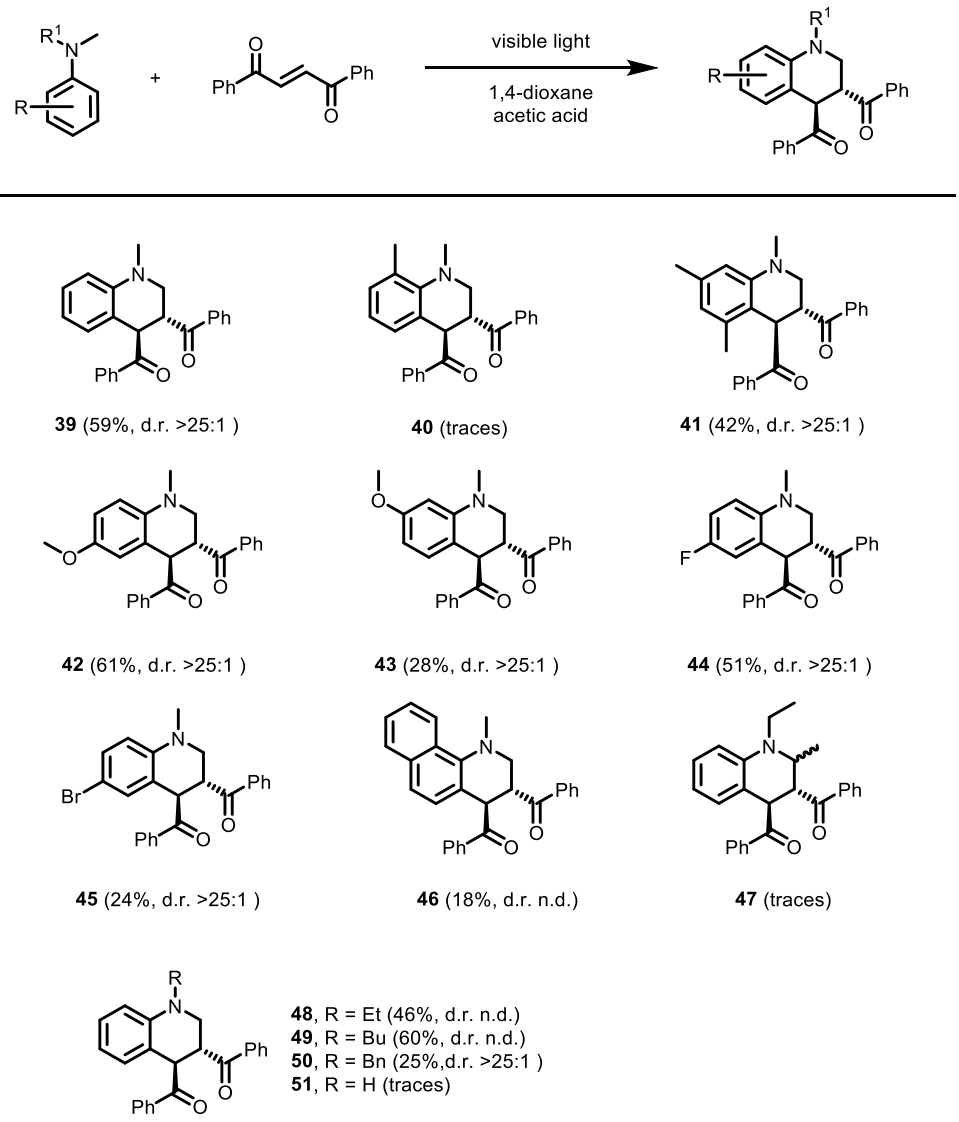

Scheme 7. Reaction scope with respect to the amine reaction partner. Rection conditions according to Table 1, entry 16. n.d. = not determined, d.r. = diastereomeric ratio.

So far, only *N,N*-dimethyl anilines were used as substrates. When *N,N*-diethylaniline was used, no product **47** could be observed. However, *N*-ethyl-*N*-methylaniline and *N*-butyl-*N*-methylaniline were compatible, giving products **48** and **49**, respectively. In these cases, only reactivity on the methyl group was observed, i.e., only the α-amino methyl radical was formed or reacted in a way giving the desired product. This observation has also been made by other authors.[49,76] A possible explanation for the selectivity is that the methyl radical reacts faster with the alkene and that its formation is faster compared to the formation of the secondary radical.[76] When a secondary aniline (*N*-H-*N*-methylaniline) was attempted as a substrate, no product could be isolated. Even though an EDA complex likely forms between the methyl aniline and the DBE, the BET after the SET is likely much faster than any productive forward process. This is a well-known problem for the α-functionalization of secondary anilines, and in chapter 6 this issue will be explained in more detail.[77]

The stereochemical outcome of the reaction favors the anti-configuration of the benzoyl groups. This was confirmed by single crystal X-ray crystallography of compound **45**, and the asymmetric unit structure, seen in Figure 10.

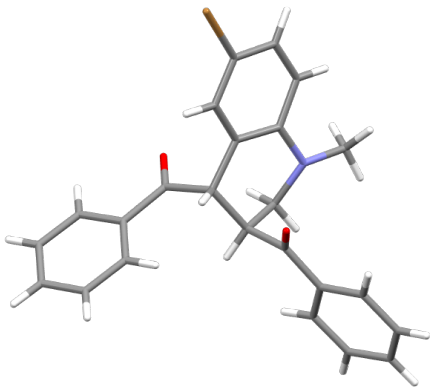

Figure 10. Asymmetric unit of compound **45**, highlighting the anti-configuration of the benzoyl moieties.

This was the case also when the *Z*-DBE was used as starting material, indicating that the reaction proceeds *via* an intermediate which enables rotation along the alkene bond (Scheme 8). If the reaction would be concerted, the *syn*-diastereomer of the product would be expected. As the *trans-cis* isomerization of DBE is well established (compare Figure 3), this feature allowed for selective formation of the *anti*-product despite the side reaction yielding the *Z*-isomer of DBE.[78]

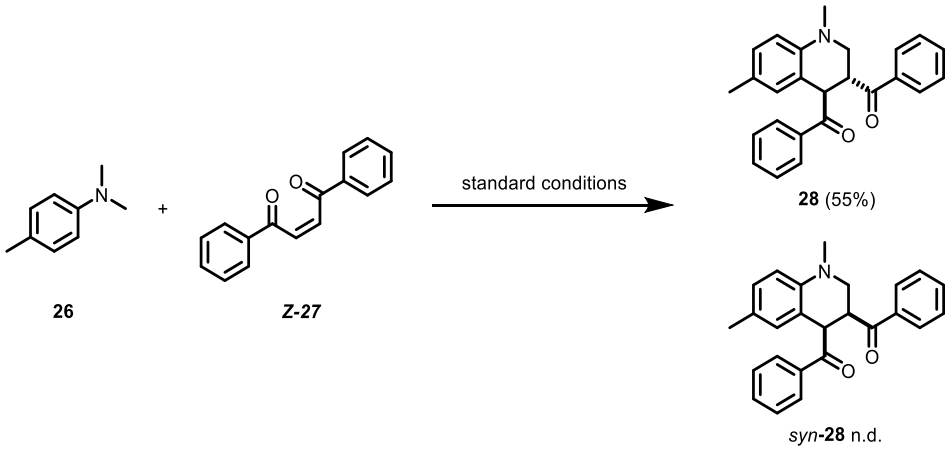

Scheme 8. Reaction between **26** and Z-**27**, leading exclusively to the anti-isomer of the product **28**.

To elucidate the mechanism of the reaction further, control experiments concluded that both light and oxygen were needed for the reaction to proceed (Table 1, entries 10 and 18). With the combined experimental results and the literature, a plausible mechanism was proposed, Scheme 9. The formation of an EDA complex was indicated by the red-shifted increased absorption occurring when mixing the aniline **26** and DBE, as can be seen Figure 9. Furthermore, titration experiments were also conducted to estimate an association constant K_a of 0.4 M^{-1}. The mechanism thus centers around the formation of an EDA complex between the dialkyl aniline and the DBE, which upon excitation with visible light leads to an enol radical (**52**) and an α-amino alkyl radical (**53**). The thermodynamic driving force for the SET in the excited complex was estimated using equation (10). The electrode potentials for **27** ($E(A/A^-)$ = -1.52 V vs SCE) and **26** ($E(D^+/D)$ = 0.72 V vs SCE), and the estimated excited state energy of **26** were used to calculate the Gibbs energy of photoinduced electron transfer to – 148 kJ/mol.[79–81] The enol radical likely reacts with molecular oxygen to reform the alkene.[31] Meanwhile, the α-amino alkyl radical adds to the alkene to form intermediate **54**, which readily cyclizes and undergoes an oxidative aromatization to yield the final product. To explain the observation of a quantum yield higher than 1, it was also postulated that the α-amino alkyl radical could to some degree form *via* the interaction of different oxygen centered

radicals formed during the course of the reaction and the aniline. This could lead to a chain propagation mechanism and has been suggested by previous studies of similar systems.[49,82] A side reaction that could also lead to the formation of **28** starts with the direct excitation of DBE. The excited DBE can then act as an electron acceptor in the reaction with **26**, effectively leading to the species **52** and **53**.

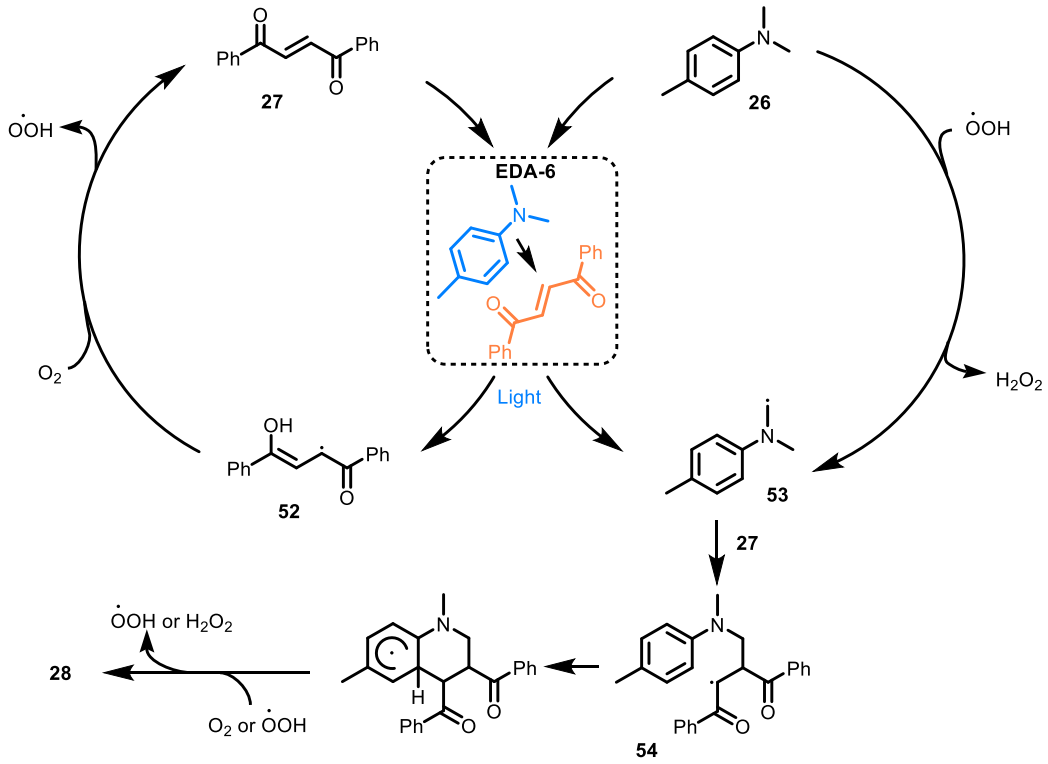

Scheme 9. Proposed mechanism.

4.3. Summary

In conclusion, we have developed a protocol for the synthesis of novel THQ derivatives using visible light irradiation. The reaction is proposed to proceed *via* the photoactivation of an EDA complex between *N,N*-dialkyl anilines as donors and 1,2-dibenzoyl ethylenes as acceptors. The excellent diastereoselectivity and the substrate scope presented shows that the method is a viable pathway to 3,4-disubstituted THQs. Furthermore, complete selectivity towards *N*-methyl activation allows for the selective construction of *N*-substituted THQs. The mild conditions, and use of aerobic oxygen as the terminal oxidant, makes the developed protocol attractive.

5. Synthesis of tetrahydroquinolines using a catalytic EDA active acceptor (Paper II)

5.1. Introduction

From the results in Paper I, it seemed that DBE was suitable for the selective oxidative activation of *N*-alkyl-*N*-methyl anilines under aerobic conditions. In order for this reaction to work, the reduced DBE (**52**) needs to be oxidized to reform the reactant **27**. This is thought to be achieved *via* the action from aerobic oxygen. This led us to the proposition that a DBE in combination with oxygen might be ideal as a catalytic system for the generation of α-amino alkyl radicals. If a suitable electrophilic radical acceptor would be present, the formed α-amino alkyl radicals could be used in a variety of different reactions. With the hypothesis that the activation of the aniline would proceed *via* the formation of a catalytic EDA complex, this would constitute one of the first examples of catalytic acceptors for EDA complex mediated organic reactions. Electron donors used in sub-stoichiometric amounts with a turnover system have been reported in several systems. Despite the many examples of external donors in EDA complex driven photoreactions, very little research has been done using catalytic acceptors in the same manner. In 2020, Ooi and coworkers reported the use of a triaryl borane as a catalytic acceptor for the net redox neutral coupling between THIQs and α,β-unsaturated ketones (Scheme 10a).[57] A second example was published in 2021, concerning the aerobic oxidative functionalization of indoles, with the same triaryl borane as catalytic acceptor (Scheme 10b).[83] However, to the best of our knowledge, no system for the oxidative coupling between amines and activated alkenes based on a catalytic acceptor had been reported.

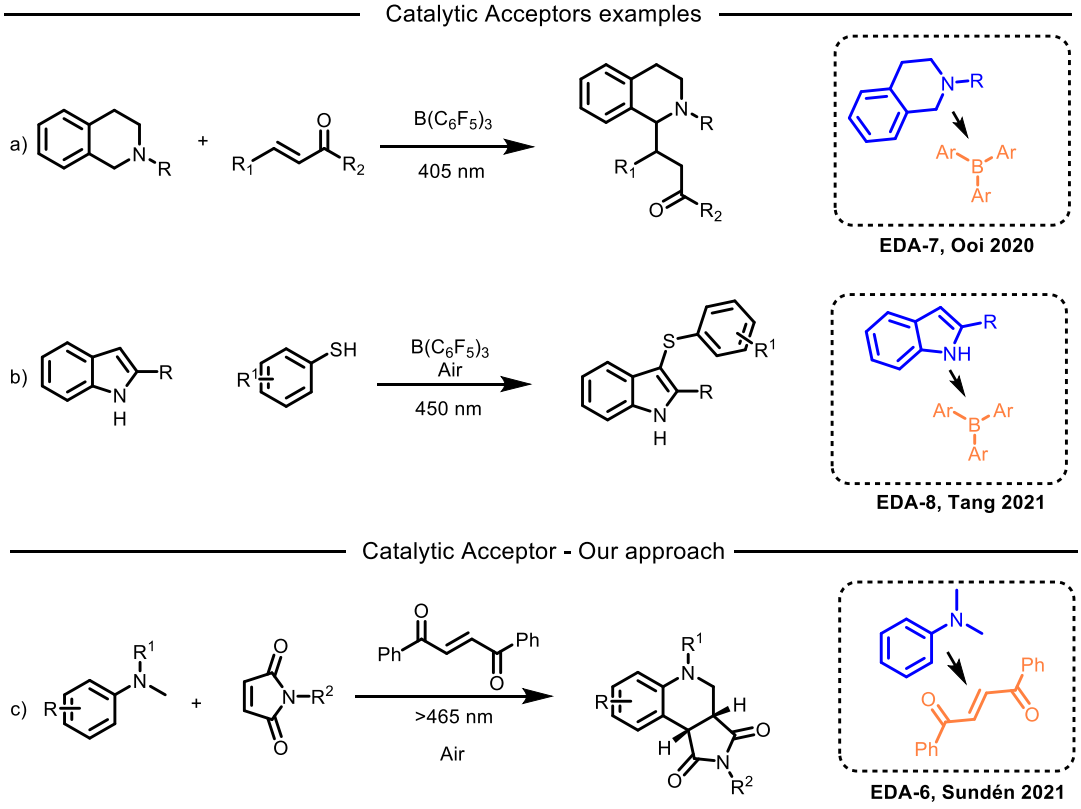

Scheme 10. Previous example of a catalytic acceptor and the proposition of the work herein; a) catalytic generation of α-amino alkyl radicals using a borane acceptor, reported by Ooi and co-workers;[57] b) aerobic oxidative sulfenylation of indoles, reported by Tang and co-workers;[83] c) this work.[41]

To test our hypothesis, a model system based on *N,N*-dimethylanilines and maleimides was chosen (Scheme 10c). It is well-established that α-amino alkyl radicals efficiently react with maleimides under a range of conditions.[31,49–54,74,84–103] Also light-induced reactions have been reported but require photocatalysts or UV-light.[31] The DBE could constitute a simpler alternative to conventional photoredox catalysts while enabling the use of visible light. Expanding the possibilities of EDA complex mediated reactions to include catalytic acceptors would also inspire further developments in the field.

5.2. Results and discussion

In this reaction, a light source consisting of a white CFL lamp was initially chosen. As it is known that dialkyl anilines and maleimides form EDA complexes that could be activated by UV-light, a background reaction without the DBE was first run.[31] It was observed that the annulation product did form to some degree, however in only 7% yield.

Table 2. Optimization of the conditions for the catalytic oxidative annulation reaction.

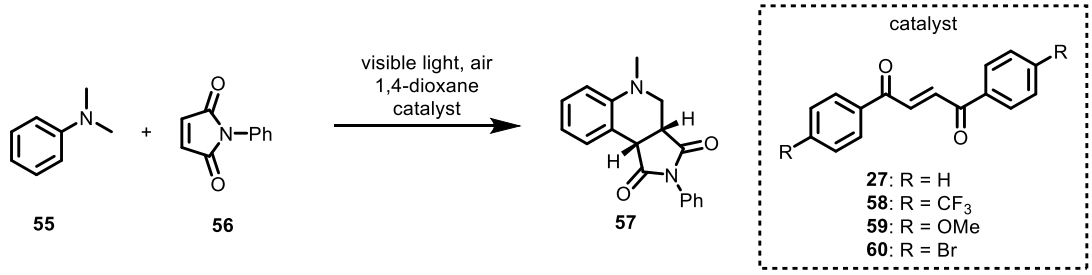

Entry	Catalyst (mol%)	Light source	Equiv. **55**	Yield **57**[b]
1	-	White CFL	7	7[c]
2	**27** (1)	White CFL	7	53
3	**27** (5)	White CFL	7	80
4	**58** (5)	White CFL	7	26
5	**59** (5)	White CFL	7	80
6	**60** (5)	White CFL	7	26
7	**27** (5)	White CFL	1	40
8	**27** (5)	White CFL	2	42
9	**27** (5)	White CFL	5	82
10	**27** (5)	-	7	12[d]
11	**27** (5)	Green LED (525 nm)	7	50[e]
12	**27 (5)**	**Blue LED (465 nm)**	**7**	**85[f] (80)[f, g]**
13	**27** (5)	Blue LED (465 nm)	7	3[f, h]

a) Conditions: **56** (0.2 mmol), **55** (1-7 equiv.) and catalyst in 3 mL 1,4-dioxane was irradiated for 6 hours under ambient atmosphere; b) determined by GC-FID using n-dodecane as internal standard; c) reaction performed in the absence of catalyst; d) reaction performed protected from light at 100 °C; e) reaction time 30 hours; f) reaction time 7 hours; g) isolated yield; h) reaction carried out under an atmosphere of nitrogen.

With addition of only 1 mol% of **27**, the yield could be increased to 53% and with 5 mol% an optimal yield of 80% could be obtained. Substituting the DBE with electron withdrawing groups on the aromatic rings resulted in inferior outcomes (Table 2, entry 4 and 6) and electron donating groups did not result in any improvements either (Table 2, entry 5). Therefore, the unsubstituted DBE **27** was chosen as the optimal catalyst for the reaction. The light source was eventually changed to a blue LED (with maximum emission at 465 nm). Green LED (525 nm) could also be used to invoke the reaction, albeit with the need of longer reaction times.

The catalytic system was then tested on a range of different maleimides in combination with **55** (Scheme 11). Generally, *N*-aryl maleimides with simple substituents were moderately tolerated giving products **62** - **65** in the range of 60-80%. Exception was *N*-(*p*-methoxyphenyl)-maleimide, yielding a sluggish reaction (Scheme 11, **64**). Introduction of a *tert*-butyl group in the *ortho* position provided the product **64** in 64% yield, and with complete diastereoselectivity due to the restricted rotation around the N-aryl bond in the maleimide moiety. The compound **64** could be heated to 180 °C to afford a mixture of the diastereomers which could easily be separated using flash chromatography.

Simple alkyl substituted maleimides reacted somewhat worse as Michael acceptors under the current conditions, resulting in lower yields of 40-60%. A trend that was observed was that bulkier *N*-substituents resulted in a higher yield (as can be seen in the series methyl, propyl, *tert*-butyl, and cyclohexyl in the compounds **67** - **70** Scheme 11).

Finally, it was concluded that other Michael acceptors than maleimides were not suitable under the current reaction conditions, as is evident from the low yields of compounds **74**–**76**. It seems like the main reason for this is the formation of a large number of unidentified byproducts, resulting in a low selectivity.

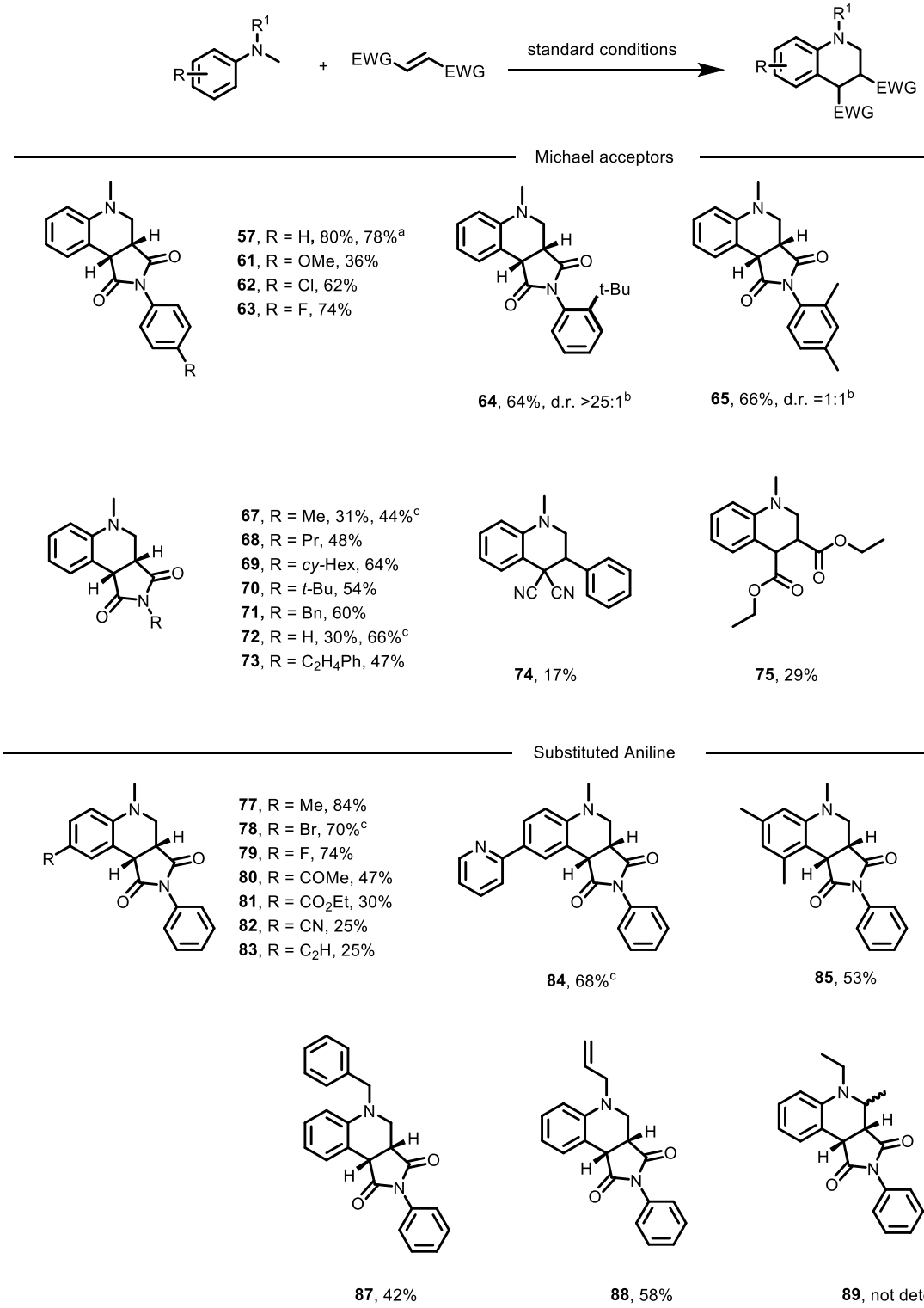

Scheme 11. Scope of the catalytic annulation reaction EWG = electron withdrawing group; a) 4.4 mmol scale; b) determined by ^{1}H NMR; c) 18 hours reaction time.

In the next series of experiments, the amine reaction partner was changed to a range of substituted dialkyl anilines. As in the case with Paper I, the electronic nature of the aniline proved to have a significant impact on the reaction outcome. Lower reaction rates were observed with electron withdrawing groups in the *para* position of the anilines, whereas electron donating groups were well tolerated. This trend was also observed in an investigation of the relative reaction rates of a series of substituted anilines (Figure 11).

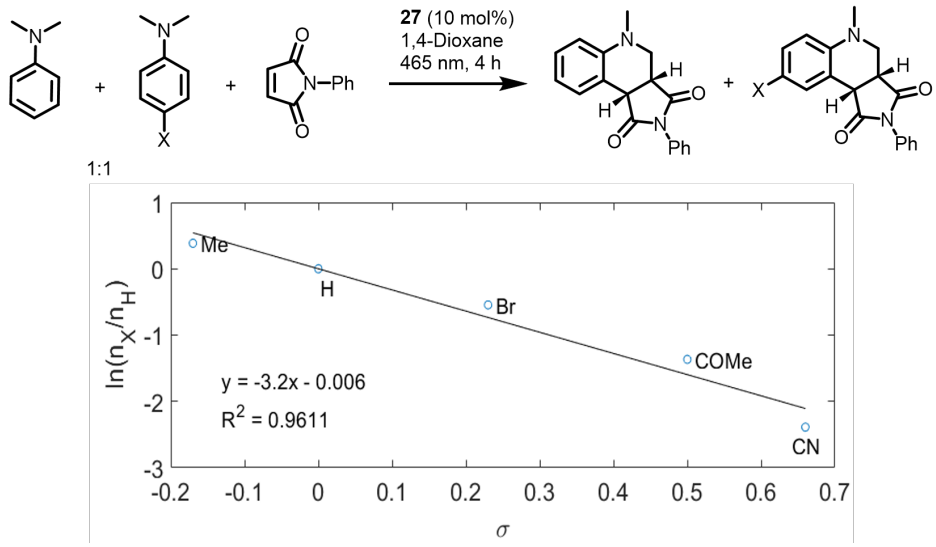

Figure 11. Relative rate of product formation as a function of the Hammett σ-parameter of substituents on the aromatic ring of the aniline reaction.[104]

Finally, similar to Paper I, when *N*-alkyl-*N*-methyl anilines were used as reactant, only reaction at the methyl group was observed, resulting in compounds **87** and **88**. The reason for this is thought to be due to the faster reaction of the methyl radical compared to the secondary alkyl radical.[76]

5.3. Investigations of the mechanism

Experiments shown in Table 2, entries 10 and 13, suggests the necessity of both light and oxygen. The reaction was also run in the prescence of the radical scavenger butylated hydroxytoluene (BHT). Under these conditions, only trace amounts of product could be obeserved, a result that points in the direction that a radical mechanism is operating. The strong influence of the electronic properties of the amine reactant suggests that a SET is involved in the rate determining step (RDS). The UV-vis study of the components in the reaction can be seen in Figure 12.

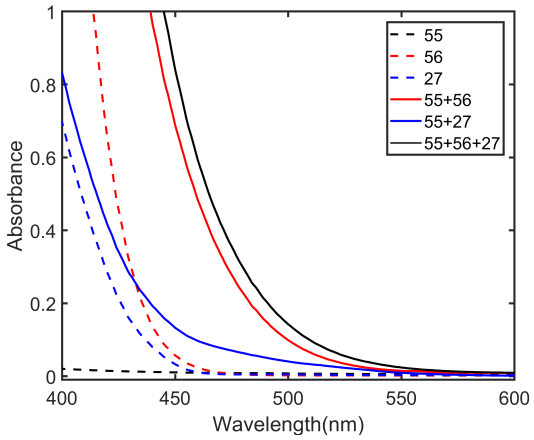

Figure 12. UV-vis spectrum of the components of the reaction and their mixtures.

From the study it is clear that the solution contains several photoactive species, and that the EDA complexes between the amine **55** and both the maleimide **56** and the DBE **27** can be excited using the 465 nm LED. To further confirm the necessity of the catalyst for the reaction, the reaction was studied over time (Figure 13). Notably, even when a 40 W 440 nm LED was used as the light source, the rate of product formation was significantly higher in prescence of catalyst. This study confirms that a background reaction is operative to some degree, but that the catalyst is necessary to drive the reaction to completion. To investigate this further, all examples in the scope were also run without the catalyst but under otherwise identical conditions (see ESI in Paper II).[41]

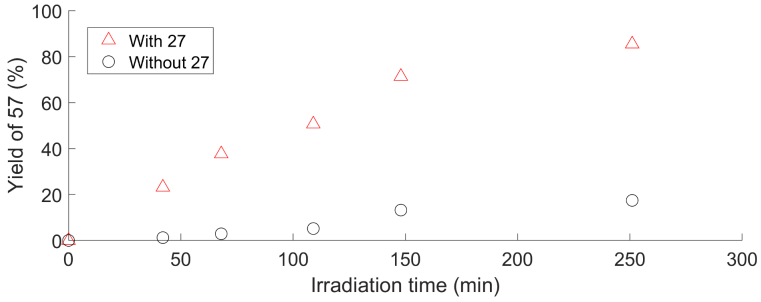

Figure 13. The yield of product **57** formed as a function of time in presence (red triangles) and absence (black circles) of the catalyst **27**. Measured by GC-FID using n-dodecane as internal standard.

As a final investigation, the effect of deuterium substitution on the aniline reaction partner was investigated. Due to the higher mass of the deuterium atom compared to the hydrogen atom, the energy barrier for C-D cleavage is higher than C-H cleavage. If the RDS of a reaction involves a C-H cleavage of some sort, the rate is therefore expected to decrease if the H is substituted for a D. A measure of this phenomena is the kinetic isotope effect (KIE), and can be expressed according to equation (14),

$$KIE = \frac{k_H}{k_D} \tag{14}$$

where k_H is the rate constant for the reaction involving C-H cleavage, and k_D is the rate constant for the reaction involving the C-D cleavage. Depending on the type of C-H cleavage, different values of the KIE can be expected.

For the functionalization of dimethylaniline developed in this paper, the question to be investigated is what role the α-C-H cleavage has in the overall reaction. Two competition experiments were therefore designed (Scheme 12). The first in which one CH_3 group of the aniline was exchanged to a CD_3 (**90**), and the second in which both CH_3 groups where exchanged (**91**). In the first experiment ("intramolecular KIE") the ratio of products **93** (resulting from C-H activation) and **92** (resulting from C-D activation) is measured. In the second experiment ("intermolecular KIE") an equimolar mixture of **91** and **55** were used as reactants. The ratio of the product **57** (resulting from C-H activation) and product **94** (resulting from C-D actviation) was then measured.

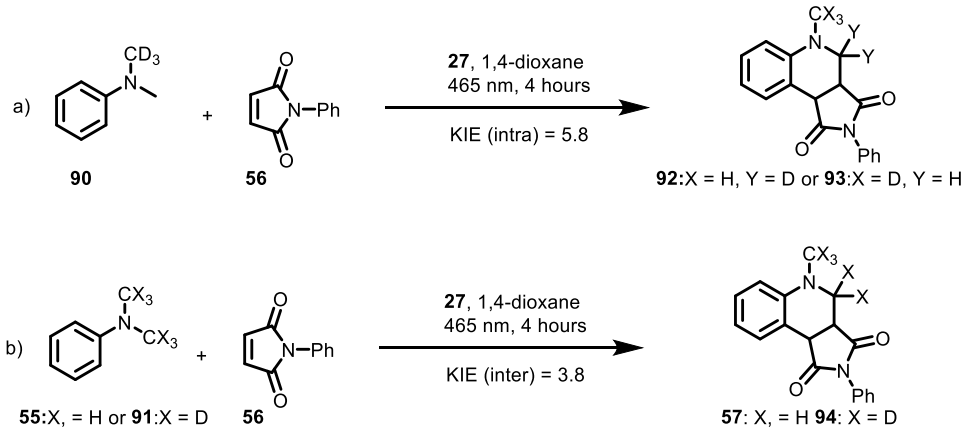

Scheme 12. Kinetic isotope effect experiments.

For the intramolecular KIE, it was observed that reaction at the CH_3 group was 5.8 times faster than the corresponding reaction at the CD_3 group. However, the intermolecular KIE observed was 3.8. These results are very similar to a previous study of a similar system.[49] The fact that an overall KIE of 3.8 was observed suggests that the C-H cleavage could have some role in the RDS. But more importantly, the difference between the intramolecular and intermolecular KIE gives some meaningful clues to the mechanism. If the reaction proceeds *via* a one-step HAT mechanism, the intra- and intermolecular KIE would be expected to be identical. However, if a two-step mechanism with similar energy barriers is operating, a difference in the two KIEs can be observed. The reaction basis for a kinetic model in the oxidative functionalization of *N,N*-dimethylanilines is outlined in Scheme 13.[105] In the two-step reaction aniline **55** is reversibly oxidized to the radical cation **95** which is then irreversibly deprotonated to the radical **96** (Scheme 13a). The observed overall reaction is presented in Scheme 13b.

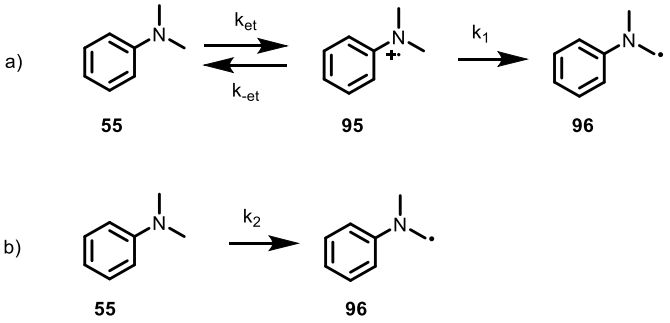

Scheme 13. The two-step formation of an amino alkyl radical.

In these reactions, the intramolecular KIE depends on the rate of the deprotonation and can be expressed as $k_{1,H}/k_{1,D}$. The intermolecular KIE will depend on the overall rate k_2, and can be expressed as $k_{2,H}/k_{2,D}$. With the assumption that the concentration of **95** is constant, the ratio

between k_1 and k_{-et} will determine k_2. Accordingly, $k_{1,H}/k_{1,D}$ and $k_{2,H}/k_{2,D}$ will be different. The relation between the two ratios can be expressed according to equation (15).[105]

$$\frac{k_{2,H}}{k_{2,D}} = \frac{k_{1,H}}{k_{1,D}}\left(\frac{k_{-et} + k_{1,D}}{k_{-et} + k_{1,H}}\right) \qquad (15)$$

Two extremes can be distinguished: $k_{-et} << k_1$ and $k_{-et} >> k_1$.[105] In the former case, the overall KIE will be equal to 1. In other words, a very slow BET compared to the deprotonation renders the SET the RDS. In the latter case, equation (15) simplifies to $k_{2,H}/k_{2,D} = k_{1,H}/k_{1,D}$, which would lead to identical intermolecular- and intramolecular KIE. In cases where BET and deprotonation occurs at similar rate, a difference in the $k_{2,H}/k_{2,D}$ and $k_{1,H}/k_{1,D}$ is observed. Importantly, the relation $k_{2,H}/k_{2,D} \leq k_{1,H}/k_{1,D}$ is always true for the system outlined in Scheme 13. With this background, the results from the KIE experiments in Scheme 12 suggest a two-step mechanism involving intermediate amine radical cation **95**.

Based on the results from the control experiment and previous reports on similar systems, a mechanism for the photoreaction was postulated (Figure 14).[31,49,60,87,95] The formation of the α-aminoalkyl radical **96** can be rationalized according to two different scenarios: either *via* direct excitation of **27**, or *via* the formation of an EDA complex between **27** and the aniline **55**. In the first case (cycle A in Figure 14), **27** absorbs a photon and is promoted to its excited state, **27***. This renders **27** a strong oxidant that can accept an electron from **55** to form the radical anion of **27** and an amine radical cation. Oxygen then intercepts the radical anion to reform **27**, whereas the radical cation is deprotonated to form an α-aminoalkyl radical. In the other scenario (cycle B in Figure 14), **27** acts as an acceptor in the GS to form an EDA complex together with the amine **55**. Excitation of this complex likewise results in the formation of the radical anion of **27** and the radical cation **95**. Deprotonation of the amine radical cation to yield the α-aminoalkyl radical can then occur within the solvent cage or after dissociation of the radical ion pair. Regardless of the mechanism, the α-aminoalkyl radical **96** then takes part in a radical addition with **56** to form a transient cyclohexadienyl radical that is readily oxidized to form the final product.

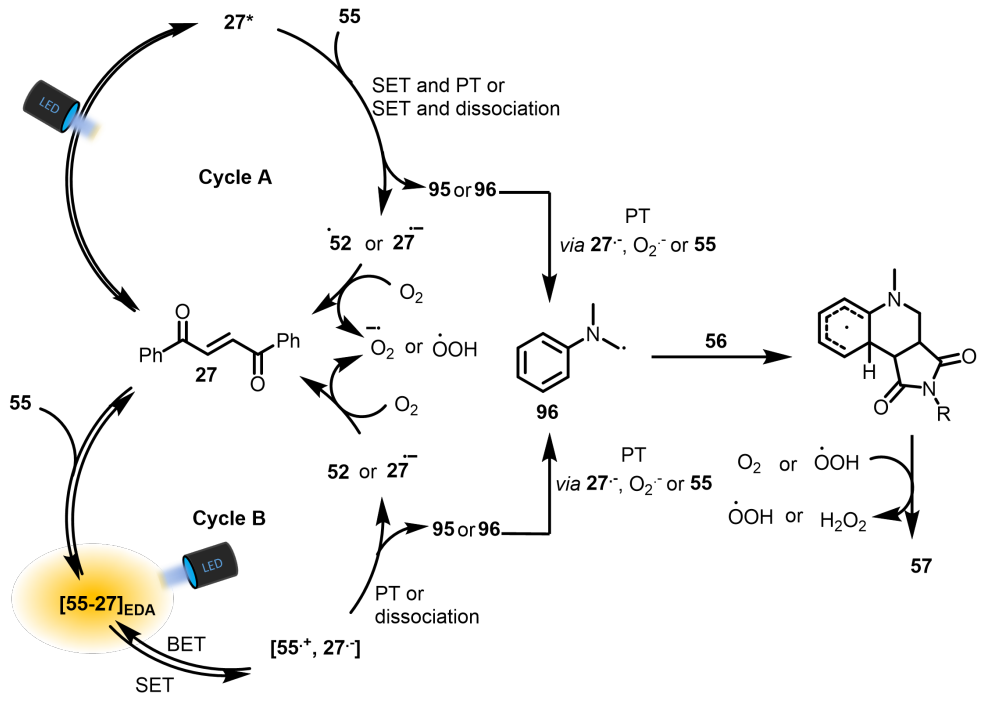

Figure 14. Proposed mechanism of the photocatalytic cycle.[41]

It is difficult to distinguish between whether cycle A or cycle B is operating. However, the observation that the reaction can be promoted, albeit with lower reaction rate, by 525 nm LED suggests that cycle B is contributing to a significant degree. At this wavelength, **27** has a low absorption compared to its EDA complex with amines (Figure 12).

5.4. Summary

In Paper II, a new photocatalytic system for the oxidative annulation reaction between *N,N*-dialkyl anilines and activated alkenes has been developed. The catalyst, 1,2-dibenzoyl ethylene, is postulated to form a photoactive EDA complex with the amine reaction partner which drives the reaction. The tetrahydroquinoline products can be formed in high yields and under mild reaction conditions using low energy light. Being a simple and available compound, the 1,2-dibenzoyl ethylene is an attractive catalyst for the type of reaction developed. Its use as a catalytic acceptor in an EDA complex driven reaction should further stimulate the field of aerobic EDA complex photochemistry in the quest of finding new reactivities.

6. EDA Complex Mediated Visible Light Driven Generation of α-Aminoalkyl Radicals from Glycines (Paper III)

6.1. Introduction

A major limitation with the methods developed in Paper I and Paper II is their inability to perform α-functionalization of secondary anilines. Albeit an EDA complex seems to form when mixing the *N*-H-*N*-methylaniline **97** and an electron acceptor, no product is observed upon irradiation of the mixture. The observation that secondary anilines are difficult to functionalize *via* oxidative activation is known in the literature.[77] One main reason behind this is thought to be the slow deprotonation of the radical cation **98** to yield **99** compared to the BET (Scheme 14).

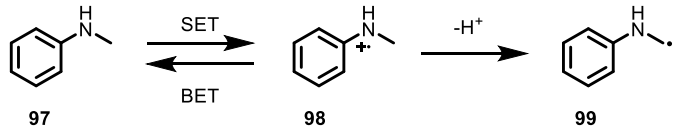

Scheme 14. Formation of an α-amino alkyl radical from a secondary aniline via a SET pathway.

This poses a problem for the otherwise facile functionalization of anilines and limits the scope of the reaction. To access secondary a-amino alkyl radicals,[§] from secondary anilines, different approaches have been employed. The installation of a better electrofuge than a proton in the α-position is a common approach. This strategy enables the formation of α-amino alkyl radicals by providing the opportunity for a more favorable fragmentation of the radical cation, hopefully competing significantly with the BET. Introduction of both silyl- and carboxyl groups has been successful in this regard.

Several examples of the photochemical activation of secondary anilines to yield α-amino alkyl radicals has been reported. However, no EDA complex mediated reactions of this type have been established. Using the knowledge gained from previous work and Paper I and III, we postulated that EDA complexes between α-carboxyl anilines and activated alkenes could work as a precursor system for the generation of secondary α-amino alkyl radicals. This method would constitute a solution to the previous limitations of the EDA complex driven activations of anilines.

[§] Secondary with respect to the aniline.

6.2. Results and discussion

As a model system for the investigation, *N*-phenyl glycine (**100**) and *N*-phenyl maleimide (**56**) were chosen. As a first step, it was established that upon mixing of the two components, a red-shifted absorption in solution was observed, Figure 15. As described earlier, this observation could be indicative of the formation of an EDA complex (Section 3.7).

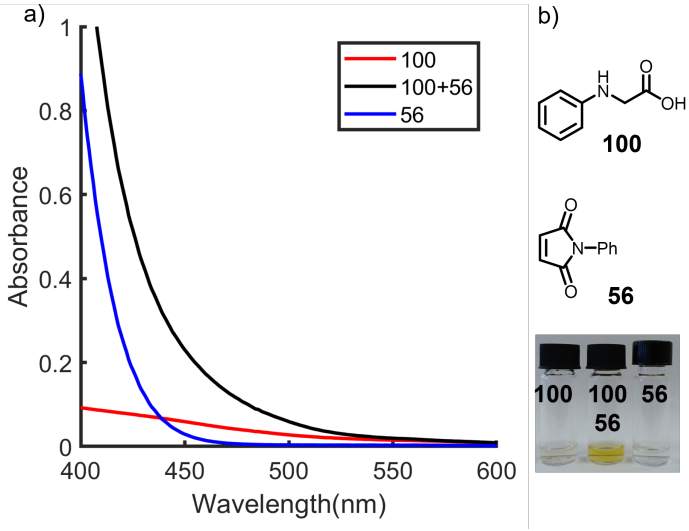

Figure 15. a) absorbance of the components **56** and **100**, and their mixture in MeOH; b) structures of **56** and **100**, and photographs showing the color change when mixing the components.

Irradiating the mixture under ambient atmosphere resulted in the formation of the desired annulation product **101**. The impacts of the reaction conditions can be seen in Table 3. It was found that a mixture of methanol and water in 2:1 ratio was the optimal solvent system, giving the product in 90% yield. Changing the solvent had a significant effect on the yield. Polar protic solvents (methanol and methanol-water) afforded high yields whereas polar non-protic solvents (acetonitrile, DMSO, 1,4-dioxane) resulted in diminishing yields. An even less polar solvent (ethyl acetate) was not suitable at all.

Table 3. Effect on the reaction conditions on the reaction outcome.

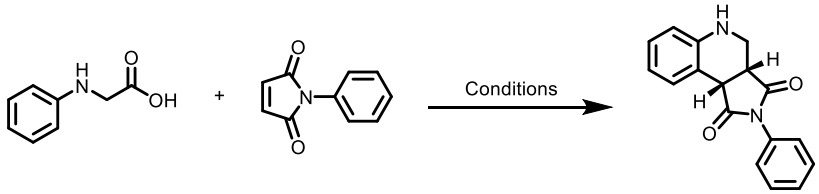

100 56 101

Entry	Deviation from standard conditions[a]	Yield **101** (%)[b]
1	none	95 (90[c])
2	EtOAc as solvent	15
3	MeCN as solvent	52
4	1,4-Dioxane as solvent	85
5	MeOH as solvent	90
6	DMSO as solvent	41
7	Green LED (525 nm), 3h	37
8	Green LED (525 nm), 18h	90
9	Under O_2 atmosphere	96
10	Under N_2 atmosphere	3
11	In the dark	0
12	UV-CFL (370 nm), 3h	34

a) Standard conditions: **56** (0.1 mmol), **100** (4 equiv.) in MeOH/H_2O (2:1) 3 mL was irradiated for 3 hours using a 440 nm 40 W LED under ambient atmosphere; b) determined by GC-FID using chlorobenzene as internal standard; c) isolated yield.

The reason for the strong solvent effect is probably very complex, and the nature of the solvent has a significant impact not only on the formation of the EDA complex and the electron transfer event, but also on the subsequent radical reactions. One interesting feature of the solvent that is worth mentioning in this context is the observation that more polar solvents result in a more red-shifted absorption (Figure 16). This goes in line with an increased stabilization of the CT state of the EDA complex in polar solvents. This made it possible to utilize green light (525 nm) as the light source, albeit with suppressed reaction rate (Table 3, entries 7 and 8).

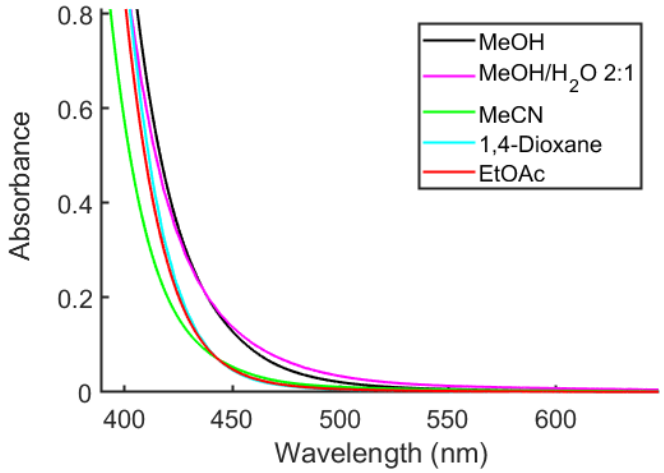

Figure 16. UV-vis absorbance of the mixture of **100** and **56** in different solvents.

As in the previous papers, once our optimized conditions were established, different substrates were tested (Scheme 15). First, different maleimides were subjected to the reaction conditions. *N*-Aryl substituents were generally well tolerated, giving compounds **101** - **106** in yields in the range of 50-90%. As in Paper II, among the *N*-alkyl maleimides a trend can be seen where more bulky groups (cyclohexyl, *tert*-butyl) resulted in higher yields.

The amine reaction partner was then investigated in terms of both substituents on the aromatic ring, α-substituents, and *N*-substituents. Reaction rates were affected by the electronic properties of the aniline, and in extreme cases, such as the *p*-cyano aniline, the reaction was too slow to efficiently result in any product. Steric hindrance through a methyl group in the *ortho* position, like in previous cases, resulted in decreased yield (compound **118**, 59%). *N*-Phenyl glycines with α-substituents resulted in lower yields, potentially due to the steric effects and/or the different properties of the intermediate α-amino alkyl radical. The introduction of another stereogenic center resulted in the formation of two diastereomers, that could only be separated in the case of α-isopropyl, compound **122**. Exchanging the *N*-H to *N*-methyl resulted in the complete selectivity towards the decarboxylated product **57**. This result highlights that the deprotonation of the α-protons is significantly slower than the decarboxylation.

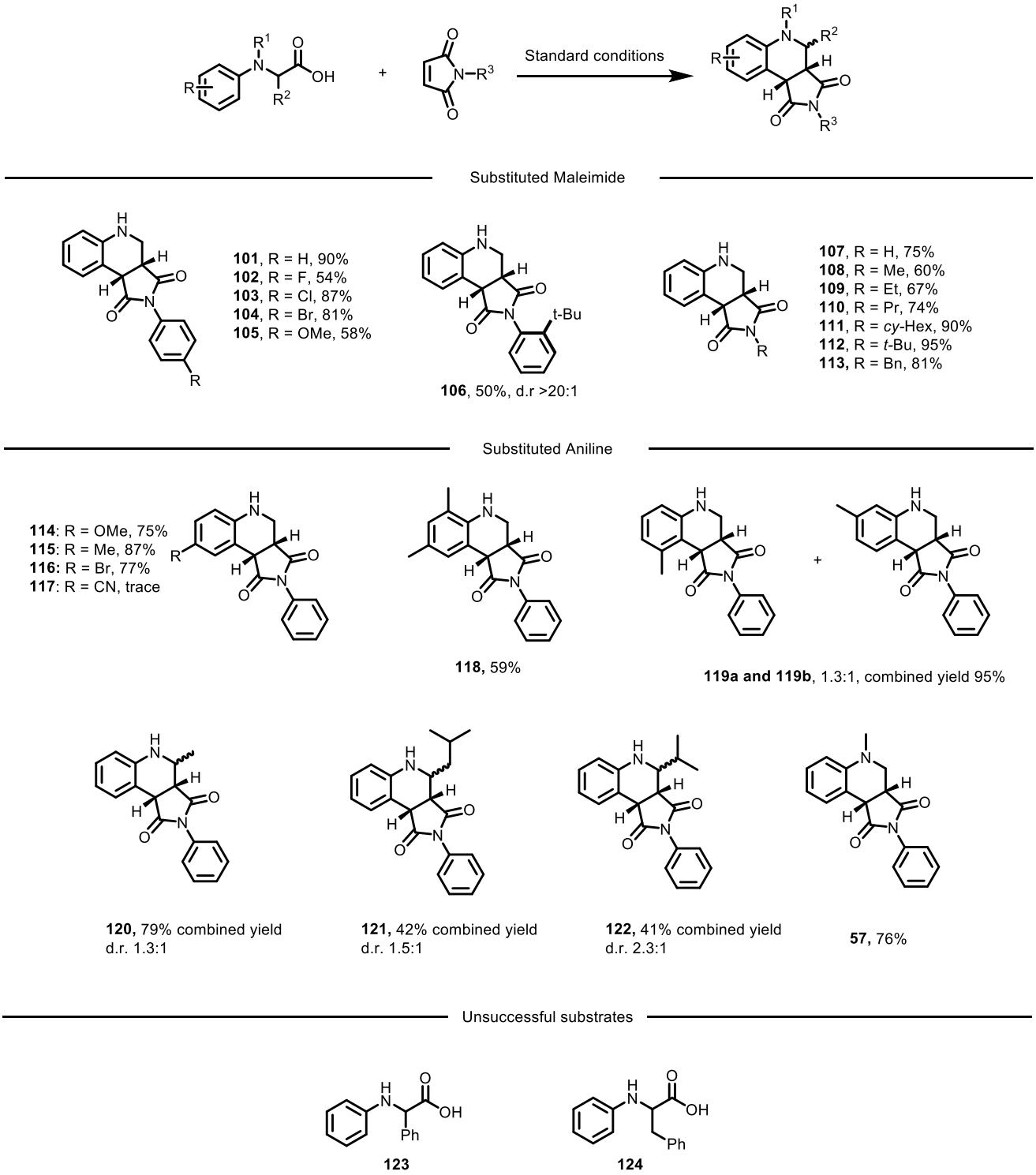

Scheme 15. Scope and limitations of the oxidative annulation reaction.

6.3. Mechanism of the reaction

The postulated mechanism for the developed reaction much resembles the mechanism from Paper I and previous work (Scheme 16).[31] Initially, an EDA complex forms between the glycine derivative and the maleimide, supported by UV-vis absorbance studies and titration experiments. Light is then absorbed by the complex, leading to the formation of a radical ion pair. Subsequently, the ion pair can either dissociate, or lead directly to a proton transfer from the glycine radical cation to the maleimide radical anion. In either case, the result is eventually a decarboxylation of the glycine and oxidation of the maleimide radical.[75,106] The formed α-aminoalkyl radical will then react with a maleimide to form the final product in the same manner as in Paper II.

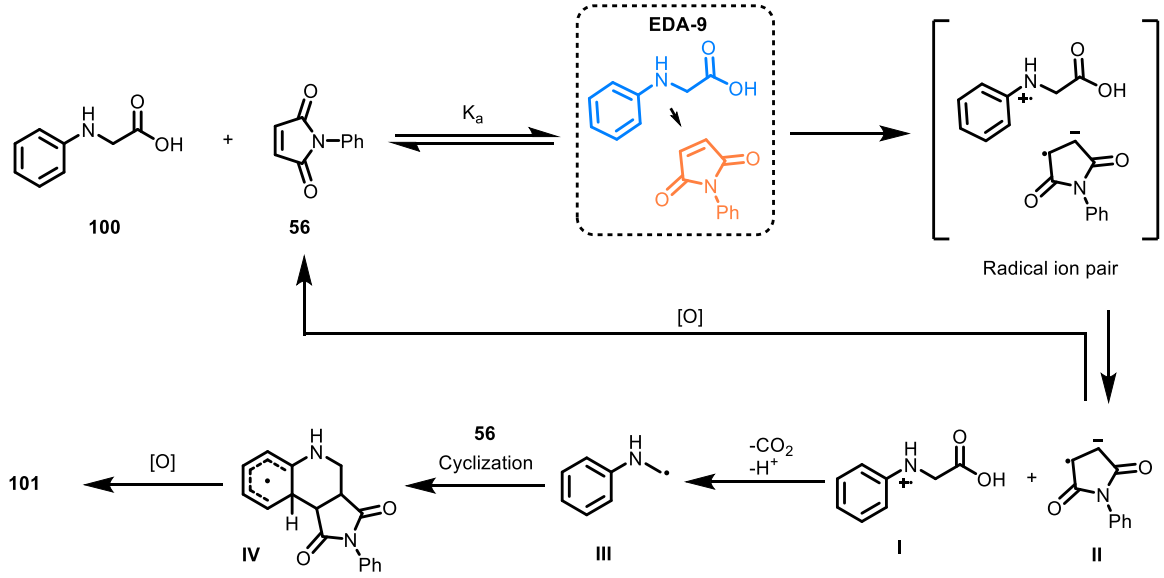

Scheme 16. Postulated mechanism for the oxidative annulation reaction.[107]

6.4. Summary

In summary, in Paper III the scope of the EDA complex mediated synhtesis of THQ was expanded to include the synhtesis of *N*-H-THQ. This constitutes an interesting extension and alternative in cases where the target THQ molecule requires a free *N*-H. The method is additive free, driven by visible light irradiation, is not moisture sensitive, and uses aerobic oxygen as the terminal oxidant – all of which make this reaction attractive from a synthetic point of view.

7. Conclusion and Outlook

In the papers herein, three new methods for the visible-light driven α-functionalization of anilines to construct compounds of the THQ family have been described. All methods also use aerial oxygen as the terminal oxidant, and all reactions are thought to proceed *via* EDA complexes as key reactive intermediates. Importantly all methods proceed using visible light as the energy source but without the need of conventional photo(redox) catalysts.

Paper I and III concerns catalyst-free methods that are thought to make use of the EDA complexes formed between the reactants directly as photoactive species. Paper II describes a new photocatalytic system based on the simple 1,2-dibenzoyl ethylene as the catalyst, which is thought to engage dialkyl anilines in EDA complexes. Apart from DBE being a simpler and cheaper catalyst, this protocol serves as a proof-of-concept to show that a catalytic acceptor can be used in the aerobic oxidative functionalization of anilines.

In Paper I, a new EDA complex between dialkyl anilines and 1,2-dibenzoyl ethylenes was identified, and a procedure for its use in the synthesis of 3,4-diaroyl-THQs was developed. It was shown that a range of different dialkyl anilines and 1,2-diaroyl ethylenes could be used in the reaction to yield the corresponding THQs in excellent diastereomeric ratios. Furthermore, complete regioselectivity towards methyl activation when employing *N*-alkyl-*N*-methylanilines was observed, providing an interesting and potentially very useful feature of the reaction. Mechanistic investigations support that the reaction proceeds *via* the photoactivation of an EDA complex, and that oxygen is needed to drive the reaction to completion. The findings in this paper expand the use of EDA complexes for the oxidative functionalization of anilines.

In Paper II, the EDA complexes identified in Paper I were used as catalysts to drive the formation of α-aminoalkyl radicals. Different alkenes were tested as radical acceptors and maleimides were found to be the most efficient. The result show that DBE cold be used as a simple and accessible catalyst for the aerobic oxidative generation of α-aminoalkyl radicals.

In Paper III one limitation of the methods developed in Paper I and II was addressed: the inability of generating secondary α-aminoalkyl radicals.[**] In order to develop a catalyst-free method to achieve this, *N*-aryl amino acids were tested as electron donors in EDA complexes in combination with maleimides. A successful method was developed to furnish 3,4-fused *N*-H-THQ in good yields. As in Paper I, the mechanistic studies supported the hypothesis that an EDA complex between the reactants might be a key photoactive intermediate in this reaction.

The findings in all three papers exemplify the use of EDA complexes for driving organic chemical reactions. Among the main features discovered is also that these reactions can efficiently be run under aerobic conditions to drive oxidations. The maleimide scaffold as an electron- and radical acceptor is well established, although more thorough investigations into the nature of the amine-maleimide complexes could be beneficial to fully understand the reactions. Of high interest would be to obtain crystal structures for these complexes, something that was attempted during the course of the project, but never accomplished. Many other EDA complexes have been observed in the investigations of the three papers described in here. Other types of activated alkenes, such as fumarates, chalcones, and nitrostyrenes, could potentially be used as electron acceptors to expand the scope of the amine-alkene complex space. However, under the aerobic conditions of main focus for this work, no successful reactions were identified. Given that the reaction mechanisms provided for the reactions presented in Paper I and III are somewhat concordant with reality, it

[**] Secondary with respect to the aniline.

can be seen that a variety of non-aerobic reactions could be designed. Introduction of other stoichiometric quenchers in the place of molecular oxygen could lead to other types of reactions, like the redox-neutral Giese addition, transfer hydrogenations and so on. This could be the next steps in the photoactivation of aniline-alkene EDA complexes and move the chemistry beyond the limited scope of the Paper I-III.

As mentioned in Section 3.7, the EDA complex driven reactions has mainly followed in the footsteps of photoredox catalysis. This has been true also for the work presented in this thesis; and although the field of EDA complex mediated reactions is by now quite mature, there might very well still be many photoredox catalyzed reactions in the literature that in fact can proceed without the catalyst – with just some minor tweaking of the reaction conditions.

8. Acknowledgements

Pursuing a PhD in organic chemistry has not been easy. My path has been accompanied with many moments of despair. Disappointments when my compounds don't behave as I want them to, failed flash columns and strange looking NMRs with a lot of grease with uncertain origin. Every organic chemist knows what I am talking about. Nevertheless, the last four and a half years have been among the most rewarding and interesting of my life. Much due to my co-workers that have been helping me through it all.

Henrik, I would like to thank you for your unstoppable energy and curiosity. For your enthusiasm and interest in all the work I have done. For the freedom that you have given me in designing my projects and engaging in a variety of others. You believe in me much more than I do myself. Thank you for sharing your knowledge in organic chemistry and for always being available for a talk about that (or about climbing of course). It has been a truly rewarding and fun time!

Jerker, thank you for being my examiner and for your support through this process, it has given me an increased confidence on several occasions!

During my time in the lab 9065, I have shared it with many great people. The "old" Sundén group made me feel very welcome and kick-started my PhD studies. I have a lot of gratitude to Anton, Chien-Wei, Bhausaheb, Claire, Linda, Mark, Martin K., and Simon J. for all your time. Since then, amazing new people have joined – Agnes, Andrea, Ellymay, Ganesh S., Ganesh G., Mario, Martin N., Martin R., you have made the PhD time much more enjoyable. Sara, it has been a pleasure and I have enjoyed all the fika, videogaming, climbing, and talks we have had. Savannah! Thank you for all your moral support, chemistry help, writing tips, proofreading, tea times, bird- and flower-talk, small adventures in town…the list can go on, but in short: you have really helped me to get through the PhD times. You are indeed a gentlewoman and a scholar. Over the years I have also had the pleasure to work with some top-notch students in my lab – thank you for all help in the projects Mathilde, Simon B., Agnes, and Camille!

Dr. Lindroth, we sort of started this together once upon a time and - although our initial plans of publishing together yet is to be realized - I think our scientific, and other intellectual, exchanges have been fruitful and valuable. I still remember the times when we genuinely enjoyed discussing chemistry for the sake of it, and it helped me a lot. But even more interesting have been the discussions (or quasi-monologues?) about whatever idea that temporarily possesses you – albeit, or perhaps because of, the high concentration of intellectual antagonism that you are able to produce.

Floor 9 has been my home basically since 2017. The number of people I have gotten the pleasure to know is vast, and I cannot include everyone here. Know however that I am very grateful for all the good times, all the fika, Julbord, tremendous amount of coffee,[††] and various shenanigans over the years. This extends to the inhabitants of the 8th floor as well. Being between two universities has some benefits, and the after-works has historically – I am sorry 9th floor – been more eventful downstairs.

Clara, thank you for all the support through my worst periods and for making the rest of the time my best.

†† Assume that I on average have had at least 3 mugs (with an approximate volume of 150 cm^3 per mug) of coffee per day since 2018-08-01. Until this day I have then consumed >725 dm^3 of coffee. Assuming an average concentration of 621 $\mu g/cm^3$ caffeine in drip-coffee,[109] I have consumed ca 0.45 kg, or 2.3 moles, of caffeine during my PhD studies.

Organic chemistry without an NMR is challenging to say the least. Therefore, I would like to express my gratitude to Bijan and Patrik for their amazing work with keeping the NMR alive.

The research presented in this thesis has been funded by grants from the Swedish research council FORMAS (2019-00699) and Wilhelm och Martina Lundgrens vetenskapliga stiftelse.

Och slutligen tack till min kära familj som alltid tror på mig och som har stöttat mig genom ökenvandringen.

9. References

1 G. E. M. Crisenza and P. Melchiorre, *Nat. Commun.*, 2020, **11**, 803.
2 P. W. Kamm, L. L. Rodrigues, S. L. Walden, J. P. Blinco, A.-N. Unterreiner and C. Barner-Kowollik, *Chem. Sci.*, 2022, **13**, 531–535.
3 N. Corrigan, M. Ciftci, K. Jung and C. Boyer, *Angew. Chemie Int. Ed.*, 2021, **60**, 1748–1781.
4 D. M. Schultz and T. P. Yoon, *Science*, 2014, **343**, 1239176.
5 M. Oelgemöller, *Chem. Rev.*, 2016, **116**, 9664–9682.
6 M. H. Shaw, J. Twilton and D. W. C. MacMillan, *J. Org. Chem.*, 2016, **81**, 6898–6926.
7 G. E. M. Crisenza, D. Mazzarella and P. Melchiorre, *J. Am. Chem. Soc.*, 2020, **142**, 5461–5476.
8 H. Sterckx, B. Morel and B. U. W. Maes, *Angew. Chemie Int. Ed.*, 2019, **58**, 7946–7970.
9 A. Gavriilidis, A. Constantinou, K. Hellgardt, K. K. (Mimi) Hii, G. J. Hutchings, G. L. Brett, S. Kuhn and S. P. Marsden, *React. Chem. Eng.*, 2016, **1**, 595–612.
10 E. Vitaku, D. T. Smith and J. T. Njardarson, *J. Med. Chem.*, 2014, **57**, 10257–10274.
11 S. E. Braslavsky, *Pure Appl. Chem.*, 2007, **79**, 293–465.
12 I. Flemming, in *Molecular Orbitals and Organic Chemical Reactions*, John Wiley & Sons, Ltd, 2009, pp. 1–67.
13 C. L. Perrin, I. Agranat, A. Bagno, S. E. Braslavsky, P. A. Fernandes, J.-F. Gal, G. C. Lloyd-Jones, H. Mayr, J. R. Murdoch, N. S. Nudelman, L. Radom, Z. Rappoport, M.-F. Ruasse, H.-U. Siehl, Y. Takeuchi, T. T. Tidwell, E. Uggerud and I. H. Williams, *Pure Appl. Chem.*, 2022, **94**, 353–534.
14 G. Andrew and J. Baggott, *Essentials of Molecular Photochemistry*, Blackwell Scientific Publications, Oxford, 1991.
15 N. J. Turro, *Modern Molecular Photochemistry*, The Benjamin/Cummings Publishing Company, Inc, 1978.
16 J. R. Bolton and M. D. Archer, in *Electron Transfer in Inorganic, Organic, and Biological Systems*, American Chemical Society, 1991, vol. 228, pp. 2–7.
17 George J. Kavarnos, *Fundamentals of photoinduced electron transfer*, VCH, 1993.
18 J. M. R. Narayanam and C. R. J. Stephenson, *Chem. Soc. Rev.*, 2011, **40**, 102–113.
19 N. A. Romero and D. A. Nicewicz, *Chem. Rev.*, 2016, **116**, 10075–10166.
20 G. B. Haxel, J. B. Hedrick, G. J. Orris, P. H. Stauffer and J. W. Hendley II, *Rare earth elements: critical resources for high technology*, 2002.
21 D. J. Cole-Hamilton, *Science*, 2003, **299**, 1702–1706.
22 S. V Rosokha and J. K. Kochi, *Acc. Chem. Res.*, 2008, **41**, 641–653.
23 C. G. S. Lima, T. de M. Lima, M. Duarte, I. D. Jurberg and M. W. Paixão, *ACS Catal.*, 2016, **6**, 1389–1407.
24 E. F. Hilinski, J. M. Masnovi, C. Amatore, J. K. Kochi and P. M. Rentzepis, *J. Am. Chem. Soc.*, 1983, **105**, 6167–6168.
25 J. K. Kochi, *Angew. Chemie Int. Ed. English*, 1988, **27**, 1227–1266.
26 R. S. Mulliken, *J. Phys. Chem.*, 1952, **56**, 801–822.
27 S. Fukuzumi, K. Mochida and J. K. Kochi, *J. Am. Chem. Soc.*, 1979, **101**, 5961–5972.
28 S. Sankararaman, W. A. Haney and J. K. Kochi, *J. Am. Chem. Soc.*, 1987, **109**, 7824–7838.
29 M. Tobisu, T. Furukawa and N. Chatani, *Chem. Lett.*, 2013, **42**, 1203–1205.
30 E. Arceo, I. D. Jurberg, A. Álvarez-Fernández and P. Melchiorre, *Nat. Chem.*, 2013, **5**, 750–756.
31 C.-W. Hsu and H. Sundén, *Org. Lett.*, 2018, **20**, 2051–2054.
32 L. Guillemard, F. Colobert and J. Wencel-Delord, *Adv. Synth. Catal.*, 2018, **360**, 4184–4190.
33 H.-W. Shih, M. N. Vander Wal, R. L. Grange and D. W. C. MacMillan, *J. Am. Chem. Soc.*, 2010, **132**, 13600–13603.
34 J. Liu, A. Guðmundsson and J.-E. Bäckvall, *Angew. Chemie Int. Ed.*, 2021, **60**, 15686–15704.

35 W. T. Borden, R. Hoffmann, T. Stuyver and B. Chen, *J. Am. Chem. Soc.*, 2017, **139**, 9010–9018.
36 N. L. Reed and T. P. Yoon, *Chem. Soc. Rev.*, 2021, **50**, 2954–2967.
37 C. K. Prier, D. A. Rankic and D. W. C. MacMillan, *Chem. Rev.*, 2013, **113**, 5322–5363.
38 W. Guo, K. Tao, Z. Xie, L. Cai, M. Zhao, W. Tan, G. Liu, W. Mei, L. Deng, X. Fan and L. Zheng, *J. Org. Chem.*, 2019, **84**, 14168–14178.
39 X. Yang, Y. Zhu, Z. Xie, Y. Li and Y. Zhang, *Org. Lett.*, 2020, **22**, 1638–1643.
40 Q. Xia, Y. Li, L. Cheng, X. Liang, C. Cao, P. Dai, H. Deng, W. Zhang and Q. Wang, *Org. Lett.*, 2020, **22**, 9638–9643.
41 A. Runemark and H. Sundén, *J. Org. Chem.*, 2022, **87**, 1457–1469.
42 K. Nakajima, Y. Miyake and Y. Nishibayashi, *Acc. Chem. Res.*, 2016, **49**, 1946–1956.
43 J. W. Beatty and C. R. J. Stephenson, *Acc. Chem. Res.*, 2015, **48**, 1474–1484.
44 C.-J. Li, *Acc. Chem. Res.*, 2009, **42**, 335–344.
45 S. A. Girard, T. Knauber and C.-J. Li, *Angew. Chemie Int. Ed.*, 2014, **53**, 74–100.
46 T. Tian, Z. Li and C.-J. Li, *Green Chem.*, 2021, **23**, 6789–6862.
47 A. G. Condie, J. C. González-Gómez and C. R. J. Stephenson, *J. Am. Chem. Soc.*, 2010, **132**, 1464–1465.
48 N. Holmberg-Douglas and D. A. Nicewicz, *Chem. Rev.*, 2022, **122**, 1925–2016.
49 X. Ju, D. Li, W. Li, W. Yu and F. Bian, *Adv. Synth. Catal.*, 2012, **354**, 3561–3567.
50 Z. Liang, S. Xu, W. Tian and R. Zhang, *Beilstein J. Org. Chem.*, 2015, **11**, 425–430.
51 J. Tang, G. Grampp, Y. Liu, B.-X. Wang, F.-F. Tao, L.-J. Wang, X.-Z. Liang, H.-Q. Xiao and Y.-M. Shen, *J. Org. Chem.*, 2015, **80**, 2724–2732.
52 Z. J. Wang, S. Ghasimi, K. Landfester and K. A. I. Zhang, *Adv. Synth. Catal.*, 2016, **358**, 2576–2582.
53 A. K. Yadav and L. D. S. Yadav, *Tetrahedron Lett.*, 2017, **58**, 552–555.
54 J.-T. Guo, D.-C. Yang, Z. Guan and Y.-H. He, *J. Org. Chem.*, 2017, **82**, 1888–1894.
55 J. F. Franz, W. B. Kraus and K. Zeitler, *Chem. Commun.*, 2015, **51**, 8280–8283.
56 C. Xu, F.-Q. Shen, G. Feng and J. Jin, *Org. Lett.*, 2021, **23**, 3913–3918.
57 Y. Aramaki, N. Imaizumi, M. Hotta, J. Kumagai and T. Ooi, *Chem. Sci.*, 2020, **11**, 4305–4311.
58 Z. Li, P. Ma, Y. Tan, Y. Liu, M. Gao, Y. Zhang, B. Yang, X. Huang, Y. Gao and J. Zhang, *Green Chem.*, 2020, **22**, 646–650.
59 Q. Xia, Y. Li, X. Wang, P. Dai, H. Deng and W.-H. Zhang, *Org. Lett.*, 2020, **22**, 7290–7294.
60 A. Runemark, S. C. Zacharias and H. Sundén, *J. Org. Chem.*, 2021, **86**, 1901–1910.
61 Z. Chen, S. Zheng, Z. Wang, Z. Liao and W. Yuan, *ChemPhotoChem*, 2021, **5**, 906–910.
62 N. Kerru, L. Gummidi, S. Maddila, K. K. Gangu and S. B. Jonnalagadda, *Molecules*, 2020, **25**, 1909.
63 V. Sridharan, P. A. Suryavanshi and J. C. Menéndez, *Chem. Rev.*, 2011, **111**, 7157–7259.
64 I. Muthukrishnan, V. Sridharan and J. C. Menéndez, *Chem. Rev.*, 2019, **119**, 5057–5191.
65 D.-S. Su, J. J. Lim, E. Tinney, B.-L. Wan, M. B. Young, K. D. Anderson, D. Rudd, V. Munshi, C. Bahnck, P. J. Felock, M. Lu, M.-T. Lai, S. Touch, G. Moyer, D. J. DiStefano, J. A. Flynn, Y. Liang, R. Sanchez, S. Prasad, Y. Yan, R. Perlow-Poehnelt, M. Torrent, M. Miller, J. P. Vacca, T. M. Williams and N. J. Anthony, *Bioorg. Med. Chem. Lett.*, 2009, **19**, 5119–5123.
66 J. Zhang, P. Zhan, J. Wu, Z. Li, Y. Jiang, W. Ge, C. Pannecouque, E. De Clercq and X. Liu, *Bioorg. Med. Chem.*, 2011, **19**, 4366–4376.
67 S. Chander, P. Wang, P. Ashok, L.-M. Yang, Y.-T. Zheng and S. Murugesan, *Bioorg. Chem.*, 2016, **67**, 75–83.
68 E. Ramesh, R. D. R. S. Manian, R. Raghunathan, S. Sainath and M. Raghunathan, *Bioorg. Med. Chem.*, 2009, **17**, 660–666.
69 R. L. Jarvest, J. M. Berge, V. Berry, H. F. Boyd, M. J. Brown, J. S. Elder, A. K. Forrest, A. P. Fosberry, D. R. Gentry, M. J. Hibbs, D. D. Jaworski, P. J. O'Hanlon, A. J. Pope, S.

Rittenhouse, R. J. Sheppard, C. Slater-Radosti and A. Worby, *J. Med. Chem.*, 2002, **45**, 1959–1962.
70 A. Muñoz, F. Sojo, D. R. M. Arenas, V. V Kouznetsov and F. Arvelo, *Chem. Biol. Interact.*, 2011, **189**, 215–221.
71 V. V Kouznetsov, D. R. Merchan-Arenas, V. Tangarife-Castaño, J. Correa-Royero and L. Betancur-Galvis, *Med. Chem. Res.*, 2016, **25**, 429–437.
72 P. Yadav and K. Shah, *Bioorg. Chem.*, 2021, **109**, 104639.
73 S. Zhu, A. Das, L. Bui, H. Zhou, D. P. Curran and M. Rueping, *J. Am. Chem. Soc.*, 2013, **135**, 1823–1829.
74 T. P. Nicholls, G. E. Constable, J. C. Robertson, M. G. Gardiner and A. C. Bissember, *ACS Catal.*, 2016, **6**, 451–457.
75 L. Chen, C. S. Chao, Y. Pan, S. Dong, Y. C. Teo, J. Wang and C.-H. Tan, *Org. Biomol. Chem.*, 2013, **11**, 5922–5925.
76 L. Leng, Y. Fu, P. Liu and J. M. Ready, *J. Am. Chem. Soc.*, 2020, **142**, 11972–11977.
77 H. Zhao and D. Leonori, *Angew. Chemie Int. Ed.*, 2021, **60**, 7669–7674.
78 K. Xu, Y. Fang, Z. Yan, Z. Zha and Z. Wang, *Org. Lett.*, 2013, **15**, 2148–2151.
79 Z. Garkani-Nejad and H. Rashidi-Nodeh, *Electrochim. Acta*, 2010, **55**, 2597–2605.
80 G. W. Dombrowski, J. P. Dinnocenzo, P. A. Zielinski, S. Farid, Z. M. Wosinska and I. R. Gould, *J. Org. Chem.*, 2005, **70**, 3791–3800.
81 Y. Ito, *Tetrahedron*, 2007, **63**, 3108–3114.
82 Q. Liu, Y.-N. Li, H.-H. Zhang, B. Chen, C.-H. Tung and L.-Z. Wu, *Chem. – A Eur. J.*, 2012, **18**, 620–627.
83 W. Yuan, J. Huang, X. Xu, L. Wang and X.-Y. Tang, *Org. Lett.*, 2021, **23**, 7139–7143.
84 Z. Almansaf, J. Hu, F. Zanca, H. R. Shahsavari, B. Kampmeyer, M. Tsuji, K. Maity, V. Lomonte, Y. Ha, P. Mastrorilli, S. Todisco, M. Benamara, R. Oktavian, A. Mirjafari, P. Z. Moghadam, A. R. Khosropour and H. Beyzavi, *ACS Appl. Mater. Interfaces*, 2021, **13**, 6349–6358.
85 Z. Xie, F. Li, L. Niu, H. Li, J. Zheng, R. Han, Z. Ju, S. Li and D. Li, *Org. Biomol. Chem.*, 2020, **18**, 6889–6898.
86 Z. Hloušková, M. Klikar, O. Pytela, N. Almonasy, A. Růžička, V. Jandová and F. Bureš, *RSC Adv.*, 2019, **9**, 23797–23809.
87 J. Li, W. Bao, Y. Zhang and Y. Rao, *Org. Biomol. Chem.*, 2019, **17**, 8958–8962.
88 X. Yang, T. Liang, J. Sun, M. J. Zaworotko, Y. Chen, P. Cheng and Z. Zhang, *ACS Catal.*, 2019, **9**, 7486–7493.
89 T. Mandal, S. Das and S. De Sarkar, *Adv. Synth. Catal.*, 2019, **361**, 3200–3209.
90 T. P. Nicholls, L. K. Burt, P. V Simpson, M. Massi and A. C. Bissember, *Dalt. Trans.*, 2019, **48**, 12749–12754.
91 K. Sharma, B. Das and P. Gogoi, *New J. Chem.*, 2018, **42**, 18894–18905.
92 X.-L. Yang, J.-D. Guo, T. Lei, B. Chen, C.-H. Tung and L.-Z. Wu, *Org. Lett.*, 2018, **20**, 2916–2920.
93 S. Firoozi, M. Hosseini-Sarvari and M. Koohgard, *Green Chem.*, 2018, **20**, 5540–5549.
94 M. Hosseini-Sarvari, M. Koohgard, S. Firoozi, A. Mohajeri and H. Tavakolian, *New J. Chem.*, 2018, **42**, 6880–6888.
95 Z. Song and A. P. Antonchick, *Tetrahedron*, 2016, **72**, 7715–7721.
96 A. K. Yadav and L. D. S. Yadav, *Tetrahedron Lett.*, 2016, **57**, 1489–1491.
97 C. Huo, F. Chen, Z. Quan, J. Dong and Y. Wang, *Tetrahedron Lett.*, 2016, **57**, 5127–5131.
98 N. Sakai, S. Matsumoto and Y. Ogiwara, *Tetrahedron Lett.*, 2016, **57**, 5449–5452.
99 M. Nishino, K. Hirano, T. Satoh and M. Miura, *J. Org. Chem.*, 2011, **76**, 6447–6451.
100 R. B. Roy and G. A. Swan, *Chem. Commun.*, 1968, 1446–1447.
101 A. M. Ranieri, L. K. Burt, S. Stagni, S. Zacchini, B. W. Skelton, M. I. Ogden, A. C. Bissember and M. Massi, *Organometallics*, 2019, **38**, 1108–1117.

102 G. Perumal, M. Kandasamy, B. Ganesan, K. Govindan, H. Sathya, M.-Y. Hung, G. Chandru Senadi, Y.-C. Wu and W.-Y. Lin, *Tetrahedron*, 2021, **80**, 131891.
103 N. F. Nikitas, M. A. Theodoropoulou and C. G. Kokotos, *Eur. J. Org. Chem.*, 2021, **2021**, 1168–1173.
104 C. Hansch, A. Leo and R. W. Taft, *Chem. Rev.*, 1991, **91**, 165–195.
105 Y. Goto, Y. Watanabe, S. Fukuzumi, J. P. Jones and J. P. Dinnocenzo, *J. Am. Chem. Soc.*, 1998, **120**, 10762–10763.
106 S. Ikeda and S. Murata, *J. Photochem. Photobiol. A Chem.*, 2002, **149**, 121–130.
107 A. Runemark and H. Sundén, *J. Org. Chem.*, 2023, **88**, 462–474.
108 A. Albini, *Photochem. Photobiol. Sci.*, 2016, **15**, 319–324.
109 R. M. Gilbert, J. A. Marshman, M. Schwieder and R. Berg, *Can. Med. Assoc. J.*, 1976, **114**, 205–208.